Nintedanib reduces corticosteroid resistance pulmonary fibrosis induced by bleomycin in mice by increasing the expression of β3 & β6 integrins

doha omar alghamdi (dohaalghamdi93@gmail.com)
King Abdulaziz University https://orcid.org/0000-0002-0820-4871
Hala S Abdel Kawy
King Abdulaziz University
zuhair A Damanhouri
King Abdulaziz University

Research Article

Keywords: pulmonary fibrosis, bleomycin, corticosteroid, resistance, combination, nintedanib

Posted Date: October 1st, 2021

DOI: https://doi.org/10.21203/rs.3.rs-899285/v2

Abstract

Background: Corticosteroid resistance pulmonary fibrosis is a major health problem. This study aimed to determine the effectiveness of nintedanib on corticosteroid resistance pulmonary fibrosis induced by bleomycin in mice.

Methods: The mice were divided into five groups 12 mice each. control group, BLM group received single dose of bleomycin (BLM), BLM+MP group received BLM and methylprednisolone (MP), BLM+NIN group received BLM and nintedanib(NIN) and BLM + NIN + MP group. The lung tissues were obtained for biochemical analysis, gene expression and histopathological examination on day 7 and day 28.

Results: after 7 days, both NIN groups showed a significant decrease in the levels of interleukin-2, interleukin-4, interferon-gamma, lung tumor necrosis factor-alpha, Malondialdehyde and lung water content with a significant increase in the Glutathione level in lung tissues compared to MP group. After 28 days, both NIN groups showed a significant reduction in hydroxyproline, and Trans-forming Growth Factor beta lung tissues contents compared to MP group, and they showed a positive effect on the expression of β 3 &β6 integrins compared to the negative effect of MP group. Histopathologically, both NIN groups showed significant improvement compared to MP group by H&E and Masson's trichrome stains. Immunohistochemical staining revealed negative BCL-2 expression in the cytoplasm of bronchiolar epithelium in both NIN groups after 7 and 28 days of treatment. Lung tissue morphometric studies showed significant improvement of pathological changes induced by BLM in both NIN groups.

Conclusions: Altogether, our data indicates that nintedanib overcame corticosteroid resistance pulmonary fibrosis induced by bleomycin.

Background

Pulmonary fibrosis is one of disease of the lower respiratory tract (Green, 2002). It may be as Idiopathic fibrosis which is unknown cause of disease or may be as a secondary effect from other causes, such as; the environmental inhalation such as; pollutants and smoking, Some typical connective tissue diseases. Infections, such as TB, SARS-CoV-2 and COVID-19, some drugs such as bleomycin, methotrexate, and Radiation therapy (Meyer, 2017).

In year of 2020, Millions of people affected by COVID-19. It is an outbreak virus affected the respiratory tract. COVID-19 induced pulmonary fibrosis resistance to corticosteroid. The risk factors of post COVID-19 pulmonary fibrosis are elderly patient, illness severity, prolong stay in ICU and patient on mechanical ventilation, smoking and chronic alcoholism (Ojo et al., 2020).

Glucocorticoid is an effective anti-inflammatory therapy for several chronic inflammatory and immune diseases, but there are several disease resistances to corticosteroid such as interstitial pulmonary fibrosis. Furthermore, the long term of corticosteroids use has been shown to be linked with a major number of comorbidities (Gross and Hunninghake, 2001). Molecular mechanisms of glucocorticoid

resistance have currently been identified. The oxidative stress leads to significantly decrease in activity and expression of HDAC2 which causes resistant to the action of glucocorticoid. Patients with glucocorticoid resistance should use alternative anti-inflammatory treatments as well as drugs that may reverse the molecular mechanism of glucocorticoid resistance (Barnes, 2010).

Bleomycin is an anti-tumour agent that produces toxicity of pulmonary tissue leading to sever progressive pulmonary fibrosis. The pathogenesis of acute pulmonary toxicity induced by bleomycin is associated with production of reactive oxygen species. The oxidants can lead inflammatory reactions in the lung. For example, the oxidation of arachidonic acid is the early step in the metabolic cascade that produces active mediators like, prostaglandins and leukotrienes. Cytokines such as IL-1, macrophage inflammatory protein-1, PDGF, and TGF- are released from alveolar macrophages of bleomycin toxicity, resulting in fibrosis. Damage and stimulation of alveolar epithelial cells may result in the release of cytokines and growth factors that stimulate proliferation of myofibroblasts and secretion of a pathologic extracellular matrix, leading to fibrosis (Hay et al., 1991). Nettelbladt and co-workers (1990) found that there is no effect of methylprednisolone treatment on bleomycin induced lung fibrosis in rat model.

The current work employed a bleomycin-induced mouse model, which is the most widely used and internationally known animal model for studying pulmonary fibrosis mechanisms (Jenkins et al., 2017). The intra-tracheal instillation of BLM in mice induces pulmonary injury characterized by an inflammatory response followed by fibrosis resembling what is happening in humans (Moeller et al., 2008, Zhao et al., 2019).

Nintedanib is an intracellular inhibitor of tyrosine kinases that targets PDGF receptors a/b, FGF receptors 1–3, VEGF receptors 1–3, TGF-b, c-Abelson and Src family kinases. Nintedanib exhibits significant therapeutic effects on modulating myofibroblast differentiation and extracellular matrix (ECM) secretion in vitro (Richeldi et al., 2014). In this study assessment of potential therapy of nintedanib either alone or combined with methylprednisolone on bleomycin induced corticosteroid resistance pulmonary fibrosis in mice was done. The present study aimed to determine the effectiveness of nintedanib on corticosteroid resistance pulmonary fibrosis induced by bleomycin in mice. No study examined the effect of nintedanib treatment in corticosteroid resistance pulmonary fibrosis induced by bleomycin and the effect of combination of nintedanib and corticosteroid to decrease the resistance to corticosteroid.

Methods

Animals:

Sixty of albino mice male adult with age of 8 to 10 weeks (20-30gram) (Kilkenny, Parsons et al. 2009). Were obtained the mice from the Animal house from pharmacy faculty, king Abdul-Aziz University, Jeddah, K.S.A. Animals were kept under a 12-hours light/dark cycle at room temperature (22±2°C) and 55±5% humidity, with provided food and water free. Under followed animal care Committee Regulations. The animals were approved by Institutional Animal Ethical Committee for King Abdul-Aziz University, faculty of pharmacy.

Drugs and chemicals:

Bleomycin sulfate powder was purchased from Shanghai Huirui Chemical Technology Co., Ltd, nintedanib powder with purity of 99% was purchased from Shanghai Huirui Chemical Technology Co., Ltd and methylprednisolone powder was purchased from Pfizer, New York were suspended in a 0.5% solution of carboxymethylcellulose sodium as a vehicle. Formaldehyde 100% was purchased from Zoad international Co for the medical supplier, KSA and di-methyl-ether was purchased from Molekula Ltd. Lingfield Way, Darlington, DL1 4XX, United Kingdom.

Mice were randomly allocated into five groups (each consisted of 12 animals) as follows:

Control group: 0.3ml of phosphate buffer saline solution by endotracheal instillation then mice were received daily oral gavage with vehicle- the vehicle was saline and 0.5% carboxymethylcellulose from day 0. 6 mice were killed at day 7 and the other 6 mice were killed at day28 (Izbicki et al., 2002).

Bleomycin group (BLM): The mice were received a single dosage (2 U/kg) in 50 µl of phosphate buffer saline by endotracheal instillation then it was received daily oral gavage with vehicle- the vehicle was saline and 0.5% carboxymethylcellulose from day 0. 6 mice were killed at day 7 and the other 6 mice were killed at day28 (Izbicki et al., 2002).

Bleomycin +methylprednisolone group (BLM+MP): BLM was endotracheal instillation. then mice were treated with 10 mg/kg methylprednisolone was prepared in fresh vehicle (0.5% carboxymethylcellulose) and dissolved in saline every day before treatment and it was administered by gavage q.d. 10mg/kg of methylprednisolone from day 0. 6 mice were killed at day 7 and the other 6 mice were killed at day28(Zhao et al., 2019).

Bleomycin +nintedanib group (BLM+NIN): BLM was endotracheal instillation. Nintedanib was prepared in fresh vehicle (0.5% carboxymethylcellulose) and dissolved in saline every day before treatment. It was administered by gavage q.d. at 60 mg/kg of nintedanib from day 0. 6 mice were killed at day 7 and the other 6 mice were killed at day28 (Wollin, Maillet et al. 2013)&(Kasam et al., 2019).

Bleomycin + methylprednisolone +nintedanib group (BLM+MP+NIN): BLM was endotracheal instillation then this group was treated by combination of nintedanib and methylprednisolone at the same previous doses.

Induction of pulmonary fibrosis by bleomycin

Anesthetize mice used a di-ethyl-ether. Load the required volume of bleomycin or sterile PBS into a sterile 200 µL pipet tip. The tongue was Pulled and extended gently using sterile padded forceps to one side, toward the mandible to visualize the vocal cords; then, lower the pipet tip loaded with bleomycin into the back of the oral cavity to deliver the liquid through the vocal cords during inspiration. Wait to hear a gasp, which confirms endotracheal delivery of the liquid. Control animals were received an equal volume of sterile PBS instead of the bleomycin solution. The tongue was released and carefully dislodge the upper

incisors from the suspension thread. The mice were placed under a heating lamp or pad until it recovers from the anesthesia(Liu et al., 2017a).

Outcome measure

After scarification the mice, the lung rapidly removed then, left lung for histological examination and right lung for analysis by ELIZA, PCR, wet/dry ratio.

Biochemical parameters measurement, after 7days post treatments

Measurement of interleukin-2 (IL-2), interleukin-4 (IL-4), interferon-gamma (INF-y), tumor necrosis factor alpha (TNFα), malondialdehyde (MDA), glutathione (GSH) contents were assessed by using the Mouse ELISA (Enzyme-Linked Immunosorbent Assay) kits is an in vitro enzyme-linked immunosorbent assay for the quantitative measurement of Mouse in Tissue Homogenates was performed as previously described(Tsoutsou et al., 2006), (Huang et al., 2010)&(Mayr et al., 2016).

The Enzyme Linked Immunosorbent (ELIZ) kits: The Mouse IL-2 ELIZA kit purchased from My-bio-source Inc. The Mouse IL-4 ELIZA kitpurchased from My-bio-source Inc. Mouse IFN-γ (Interferon Gamma) ELISA Kit purchased from My-bio-source Inc. Abcam's tumor necrosis factor alpha Mouse ELISA (TNF-α): TNF-α Immunoassay ELISA purchased from Abcam's Co. Mouse malondialdehyde (MDA) ELISA Kit (competitive ELIZA) purchased from My-bio-source Inc. GSH(Glutathione) ELISA Kit in mice purchased from Elab-science Co.

Biochemical parameters measurement, after 28 days post treatments

Measurement of transforming growth factor beta (TGF-β) and hydroxyproline contents were assessed by using the Mouse ELISA (Enzyme-Linked Immunosorbent Assay) kits is an in vitro enzyme-linked immunosorbent assay for the quantitative measurement of Mouse in Tissue Homogenates was performed as previously described(Sisson et al., 2010)&(Saraiva et al., 2018). The Enzyme Linked Immunosorbent (ELIZ) kits: Lung Transforming growth factor-β1 (TGF-β1) in mice purchased from Picokine Co. Bio-vision's hydroxyproline ELISA Kit in mice purchased from bio-vision's Inc.

Tissue homogenate

The lung tissue rinsed in ice-cold PBS (0.01M, pH=7.4) to eliminate excess blood thoroughly. The 100mg tissue was rinsed with 1x PBS, homogenized in 1 ml of 1x PBS and stored immediate at -20°C. Next of two freeze-thaw cycles were performed to break the cell membranes, the homogenates were centrifuged for 5 min at 5000×g at 2 - 8°C to get the supernatant for immediately assayed or stored at -20°C or -80°C to avoid loss of bioactivity and contamination. Centrifuge the samples again before the assayed. Avoid multiple freeze-thaw cycles.

Wet-to-dry lung weight ratio at day 7 & at day 28 post-treatments:

The lung wet-to-dry (W/D) weight ratio was used as an index of lung water accumulation after endotracheal instillation of bleomycin. To measure the lung water content and edema, the animals were killed under deep ether anesthesia, and the lung weight was measured directly after its removal (wet weight). The lung tissue was then dried in an oven at 60°C for 5 days and re-weighed as dry weight. The W/D weight ratio was calculated by dividing the wet by the dry weight(Matsuyama et al., 2008).

Gene expression of β3and β6 integrins profiling by real-time quantitative polymerase chain reaction (qPCR) at day 28 post treatment:

Lung tissue was removed from each mouse using a dissecting scissor and forceps. The dissecting was performed by the same investigator for all animals to limit discrepancy in the sample collection. Tissue from three mice was pooled for each biological replicate (12 animals per group were used to obtain 3 biologicals replicates). The lung tissues were transferred to liquid nitrogen directly. Lung tissue was homogenized in a homogenizer on ice and total RNA was isolated using Thermo Scientific GeneJET RNA Purification Kit #K0731 (USA). RNA samples with 1.8 to 2.0 of OD260/280 ratio were accepted for analysis. 1 µg of total RNA was reverse-transcribed using High-Capacity cDNA Reverse Transcription Kits (Applied Biosystems, USA). RT-qPCR was performed as previously described (Bi et al., 2016, Bi et al., 2019).

Showed the sequences of gene of Integrins b3 &b6

Mouse Gene	Orientation	Sequence
Itgb3	Forward	CTAGCAACCTTCGGATTGGC
	Reverse	CAGCACGTGTTTGTAGCCAA
Itgb6	Forward	AAAACCCTGTCTCCCGCATA
	Reverse	AATCTTCAGTTTGGCGGACC

Showed the references of mouse gene

Mouse Gene	Orientation	Sequence
GAPDH	Forward	CATTGTGGAAGGGCTCATGG
	Reverse	AGGTGGAAGAGTGGGAGTTG

Lung histopathology:

The left lung specimens from each animal were fixed in 10 % formalin solution. Fixation was followed by dehydration, clearing, and embedding in paraffin. Serial sections of 5 µm thickness were cut then stained using the following stains and measurements were performed by a pathologist blinded to the study groups. H&E and trichrome blue slides were reviewed and subjectively analyzed for general signs of

inflammation and fibrosis. As the same mentioned in histological analysis and lung damage severity scores acute after one week and chronic after 4 weeks (Aubin Vega et al., 2019)&(Polosukhin et al., 2012). Visualization and photographing of slides were done using an Olympus light BX61microscope.

Immuno-histochemical analysis for BCL-2 at day 7 & at day 28 post-treatment:

The left lung specimens from each animal after one week and after 4 weeks of bleomycin and treatment administration were fixed in 10 % formalin solution. Fixation was followed by dehydration, clearing, and embedding in preparation of 5um paraffin section slides. Immuno-histochemical technique for detection of Bcl-2 expression was performed using labeled streptavidin biotin technique (Zymed) Cat No. 18-0193 with the monoclonal antibody (Bcl-2). The localization of Bcl-2 protein was demonstrated as yellowish brown color area(Ahmed and Anwar, 2004).

Morphometric measurement after 7 days, the mean thickness of the interalveolar septa in (µm) and the mean alveolar space surface area (µm 2) after 7 days As the same mentioned in morphometric analysis (Zakaria et al., 2021). Blind histological analysis was performed on the lung paraffin sections from mice after 7 days for estimation of parenchymal distortion and airway (peribronchial) inflammation using specific semi-quantitative scores: Analysis of Lung parenchymal distortion: It was assessed by analysis of ten sequential non-overlapping tissue fields using x200 magnification. Each tissue field was scored using a 0-to-4-point system. Mean scores for all fields were calculated for each mouse (Polosukhin et al., 2012). Analysis of airway inflammation: It was estimated by individual assessment of each airway in the tissue section using a 0-to-3- point system. Mean scores for all analyzed airways were calculated for each animal (Polosukhin et al., 2012).

Measurement of area percentage of PCL-2 immunostaining after 7 days.

The intensity of immunohistochemical staining was graded semiquantitative as follows: grade 0 = no staining present or less than 10% of the cells are positive; grade 1 = 10% of the cells are positive; grade 2 = more than 10% and less than 50% of the cells are positive and grade 3 = more than 50% of the cells are positive (Safaeian et al., 2008).

Morphometric analysis after 28 days: measurement of the area percent of collagen fibers in Masson trichrome stain as same mentioned (Zakaria et al., 2021).They were measured by using the NIH Image J (v1.50) program and measurement of subepithelial connective tissue volume density (VVsub) in Masson trichrome stain after 28 days. Airway wall remodeling was evaluated by measurement of VV sub as the difference in the area, delimited by the basement membrane and the outer edge of the airway adventitia, divided by the length of subepithelial basement membrane (Polosukhin et al., 2012). They were measured from x 40 photomicrographs using Digimizer 4.3.2. image analysis software (MedCalc Software bvba, Belgium).

Statistical analysis

Statistical comparisons among experimental groups were performed by one way of variance (ANOVA) followed by Tukey's multiple. Student's t-test for paired comparisons was performed. The log2-transformed data was used for the RT-qPCR statistical analysis (Rieu and Powers 2009). The values were presented as mean± standard error of mean (SEM). The proportion of the lung tissues present was analyzed by Fisher's exact test. $P < 0.05$ was considered statistically significant. All analyses were used SPSS 25.0 statistical software (IBM Corp., Armonk/ N.Y., USA). Significant differences between experimental groups were determined at P. value <= 0.05. The graphs were made by using prism version.9 Correlations between measured parameters were made using Pearson correlations. P. values < = 0.05 were considered significant.

Result

The effect of nintedanib (NIN) and methylprednisolone (MP) either alone or in combination on inflammatory markers and cytokines contents in lung tissue in a mice model of corticosteroid resistance pulmonary fibrosis induced by bleomycin after 7-days post treatments:

Figure 1 showed significant reduction in the contents of IL-2, IL-4, INF-gamma and TNF-α in bleomycin group treated with NIN either alone or combined with MP compared to bleomycin group treated with MP ($P < 0.05$). No significant differences were detected between the bleomycin treated group with NIN either alone or combined with MP.

The effect of nintedanib (NIN) and methylprednisolone (MP) either alone or in combination on oxidative stress contents in lung tissue in a mice model of corticosteroid resistance pulmonary fibrosis induced by bleomycin after 7-days post-treatments:

Figure 2 showed significant reduction in the content of MDA in bleomycin group treated with NIN alone or in combined with MP compared to bleomycin group treated with MP alone and it showed significant increase in the content of GSH in bleomycin group treated with NIN alone or in combined with MP compared to bleomycin group treated with MP alone($P < 0.05$). No significant differences were detected between the bleomycin treated group with NIN either alone or combined with MP.

The effect of nintedanib (NIN) and methylprednisolone (MP) either alone or in combination on transforming growth factor beta and hydroxyproline contents in lung tissue in a mice model of corticosteroid resistance pulmonary fibrosis induced by bleomycin after 28-days post treatments:

Figure 3 showed significant reduction in the contents of TFG-β and hydroxyproline in bleomycin group treated with NIN alone or in combined with MP compared to bleomycin group treated with MP alone ($P < 0.05$). No significant differences were detected between the bleomycin treated group with NIN either alone or combined with MP.

The effect of nintedanib and methylprednisolone either alone or in combination on the lung water content in lung tissue in a mice model of corticosteroid resistance pulmonary fibrosis induced by bleomycin after

seven (7) & 28 days post treatments:

figure 4 showed significant decrease in the content of water in the bleomycin group treated with MP, bleomycin group treated with NIN and the bleomycin group treated with NIN+ MP compared to bleomycin group at p. value <0.05. No significant difference between the bleomycin group treated with MP and bleomycin group treated with NIN and the bleomycin group treated with NIN+ MP after 7 days post-treatments.

Figure 4 showed significant reduction in the contents of water in bleomycin group treated with NIN alone or in combined with MP compared to bleomycin group treated with MP alone. No significant difference between the bleomycin group treated with MP and bleomycin group. No significant difference between the bleomycin group treated with MP and bleomycin group treated with NIN and the bleomycin group treated with NIN+ MP after28 days post-treatments.

The effect of nintedanib (NIN) and methylprednisolone (MP) either alone or in combination on gene expression of β3 & β6 integrins compared to control group and bleomycin group in lung tissue in a mice model of corticosteroid resistance pulmonary fibrosis induced by bleomycin 28-days post-treatments:

Figure 5 showed the negative effect of bleomycin group on wound healing was associated with a significant decrease in the expression of β3 & β6 integrins compared to control group at p. value <0.00. Also, it showed the bleomycin group treated with MP, bleomycin group treated with nintedanib, and the bleomycin treated with (MP+NIN) downregulation of the expression of β3 & β6 integrins compared to control group **in addition** there was downregulation in β3 integrin gene in the bleomycin group treated with MP compared to bleomycin group but upregulation in β3 & β6 integrins gene in the bleomycin group treated with NIN and the bleomycin treated with (MP+NIN) compared to bleomycin group.

Histological Results after 7 days post treatments:

Hematoxylin and eosin (H&E) stained sections

(Control group): lung sections revealed numerous alveolar sacs, the alveoli appeared patent with thin interalveolar septa. The bronchioles showed folded mucosa covered with simple columnar ciliated epithelium. Clara cells occasionally appeared in between the epithelial lining of the bronchioles with their dome shaped apices. Lamina propria was seen under the epithelium. Bundles of smooth muscles and adventitia were also noticed surrounding the mucosa. The alveolar ducts and alveoli were lined with simple squamous epithelium and thin rim of lamina propria. The alveolar epithelium was formed of both type I and type II pneumocytes. Type I pneumocytes were flat cells with flattened nuclei and attenuated cytoplasm. Type II pneumocytes appeared rounded or cuboidal in shape with large, rounded nuclei and vacuolated cytoplasm. They were commonly located in the corners of alveolar septa and showed rounded apical surface projecting above the level of the surrounding epithelium. Thin interalveolar septa were observed between the alveoli, it consisted of alveolar epithelia, capillaries, and delicate connective

tissue. The interstitial tissue of the lung contained branches of pulmonary artery and vein (Figs6. 1A & 2A). **(BLM group):** revealed marked distorted bronchiole with obliteration of the lumen. Moreover, most of bronchial passages were seen surrounded by marked aggregation of mononuclear cells and marked inflammatory cellular infiltration in the adventitia of bronchioles were observed. The epithelial lining of the bronchial passages showed marked disorganization and degeneration in which their epithelial lining exhibited vacuolation. Their lumen appeared obliterated by desquamated and exfoliated epithelium. Also, cellular aggregates detected in marked thickened inter-alveolar septa. Notice marked obliteration of most alveoli with some alveoli appear collapsed and widening of other alveoli were seen. Congested dilated blood vessels with thickened wall were noticed in all sections (Figs6. 1B & 2B). **(BLM+MP):** revealed marked distorted bronchiole with partially obliteration of the lumen. Moreover, most of bronchial passages were seen surrounded by marked aggregation of mononuclear cells. The epithelial lining of the bronchiolar passages showed marked disorganization and degeneration in which their epithelial lining exhibited vacuolation with eukaryotic nuclei. Their lumen appeared obliterated by detached epithelial cells. Moreover, massive cellular aggregates detected in marked thickened inter-alveolar septa. Notice marked obliteration of most alveoli with focal areas of collapsed alveoli with compensatory dilatation of neighboring ones. Massive congested dilated blood vessels with thickened wall were noticed in most of the stained sections. Eosinophilic exudates and extravasations of red blood cells in the inter-alveolar septa were frequently seen (Figs6. 1C & 2C). **(BLM+NIN)** showed moderate improvement of lung architecture, but not full complete histological recovery as compared to control group. The lung sections revealed some bronchioles with vacuolated epithelial cells along with normal lining epithelium, moderate inflammatory cell infiltration in the moderately thickened septa, around alveoli and bronchioles, few thickened blood vessels wall. Notice most of the alveoli are apparent nearly as a control group (Figs6. 1D & 2D). **(BLM+MP+NIN)** exerted an ameliorating effect on the lung structure. There were few focal areas of inflammatory cellular infiltration that were noticed surrounding the bronchi. Moreover, the lining epithelium of the bronchi was nearly comparable to that of the control group. Notice most of the alveoli are apparent nearly as a control group with thin inter-alveolar septa (Figs6. 1E & 2E).

Masson's trichrome stain:

Examination of mice lung sections of **(control group)** revealed few collagen fibers in the perivascular areas. Scanty collagen fibers in the interalveolar septa and around bronchiolar passages were evident as well (Fig7. 1A). While **(BLM) and (BLM+MP)** exhibited an apparent increase of collagen fibers deposition in the lung interstitium, in areas surrounding the bronchioles (denoting lung fibrosis), and surroundings the alveoli as compared to that in control group (Figs7. 1B & 1C). Meanwhile, sections of **(BLM+NIN)** showed an apparent decrease of collagen fibers in the interalveolar septa as well as around the bronchi (Fig7. 1D). While, in **(BLM+MP+NIN)** some collagen fibers were seen in the interalveolar septa as well as around the wall of bronchi (Fig7. 1E). Nearly both BLM+NIN and BLM+MP+NIN groups appeared as control group.

Immunohistochemical analysis for BCL-2

In immunohistochemical analysis for BCL-2, sections from the **control group** showed very few cells with positive immune reaction in the cytoplasm of alveolar epithelium lining of the alveoli and bronchiolar epithelium. Notice a few strong positive reactions in the interstitial tissue in the lumen of some alveoli (Fig7. 2A). However, in **(BLM group) and (BLM+MP)** most of the cells with strong positive immune reaction were seen in inter-alveolar septa and the interstitium of the lung. Few positive immune reactions were seen in the epithelium lining the bronchial lumen (Figs7. 2B & 2C). Meanwhile, in **(BLM+NIN)**, few cells with strong positive BCL-2 immune reaction were seen in the inter-alveolar septa (Fig7. 2D). Also, sections of **(BLM+MP+NIN)** showed few cells with strong positive immune reaction for BCL-2, in inter alveolar septa. Notice negative BCL-2 positive brownish expressions of the cytoplasm of bronchiolar epithelium were seen in both BLM+NIN and BLM+MP+NIN groups (Fig7. 2E).

Histological Results after 28 days:

Hematoxylin and eosin (H&E) stained sections

(Control group) lung sections revealed the same histological pictures of control group after 7 days (Figs8. 1A & 2A). **(BLM group)** revealed massive, distorted bronchiole with marked loss of architecture of the bronchiole. Most of the bronchiole appeared with marked cellular debris in the lumen, marked inflammatory cellular infiltration in the interstitial tissue and surrounding the bronchiole, and congested dilated blood vessel were seen. Notice obliteration of most alveoli with some alveoli appeared collapsed and widening of other alveoli. Marked eosinophilic exudate in the septa and around alveoli and many extravasations of RBCs were observed in most of the sections. Moreover, most of the bronchiolar passage exhibited thick muscle layer. The epithelial lining appeared vacuolated with darkly stained pyknotic nuclei. Notice markedly thickened inter-alveolar septa studded with heavy cellular infiltration were seen. Notice pneumocytes type I and cuboidal pneumocytes type II appeared with deeply stained pyknotic nuclei. The eosinophilic exudate and many extravasations of RBCs were markedly seen in most of the sections (Figs8. 1B & 2B). **(BLM+MP)** revealed that most of the epithelial lining of the bronchiolar passage appeared vacuolated with eukaryotic nucleus with multiple area of eosinophilic red materials. Notice extravasations of RBCs and heavy cellular infiltration in the form of lymphocytes, neutrophil, and multinucleated giant cells in thickened interalveolar septa around the alveoli were seen. Moreover, marked obliteration of most of the alveoli, some appeared collapsed, and some showed widening of the lumen. Massive congested dilated blood vessels with thickened wall were noticed in most of the stained sections. Eosinophilic exudates and extravasations of red blood cells in the inter-alveolar septa were frequently seen. In some sections exhibited marked cellular acidophilic structures with spindle shape, marked eosinophilic exudate with large focal rounded zone of inflammatory cells, and many extravasations of RBCs were seen (Figs8. 1C & 2C). **(BLM+NIN)** showed mild improvement of lung architecture, but not full complete histological recovery as compared to group I (control group). The lung sections revealed some bronchioles with vacuolated epithelial cells along with normal lining epithelium, few focal areas of inflammatory cell infiltration in the moderately thickened septa, around alveoli and bronchioles, few thickened blood vessels wall. Notice most of the alveoli are apparent nearly as control

group (Figs8. 1D & 2D). (**BLM+MP+NIN)** exerted an ameliorating effect on the lung structure. There were few focal areas of inflammatory cellular infiltration were noticed surrounding the bronchi. Moreover, the lining epithelium of the bronchi was nearly comparable to that of the control group. Notice most of the alveoli are apparent nearly as control group with thin inter-alveolar septa (Figs8. 1E & 2E).

Masson's trichrome stain:

Examination of mice lung sections of **(control group)** revealed few collagen fibers in the perivascular areas. Scanty collagen fibers in the interalveolar septa and around bronchiolar passages were evident as well (Fig9. 1A). While **(BLM group) and (BLM+MP)** exhibited an apparent increase of collagen fibers deposition in the lung interstitium, in areas surrounding the bronchioles (denoting lung fibrosis), and surroundings the alveoli as compared to that in control group (Figs9. 1B & 1C). Meanwhile, sections of **(BLM+NIN)** showed an apparent decrease of collagen fibers in the interalveolar septa as well as around the bronchi (Fig9. 1D). While, in **(BLM+(MP+NIN))** some collagen fibers were seen in the interalveolar septa as well as around the wall of bronchi (Fig9. 1E). Nearly both BLM+NIN and BLM+MP+NIN groups appeared as control group after 28 days.

Immunohistochemical analysis for BCL-2

In immunohistochemical analysis for BCL-2, sections from the **(control group)** showed very few cells with positive immune reaction in the cytoplasm of alveolar epithelium lining of the alveoli and bronchiolar epithelium. Notice few strong positive reactions in the interstitial tissue in the lumen of some alveoli (Fig.9.1A). However, in **(BLM group) and (BLM+MP)** most of the cells with strong positive immune reaction were seen in inter-alveolar septa and the interstitium of the lung. Marked positive immune reaction were seen in the epithelium lining the bronchiole lumen (Figs9. 1B & 1C). Meanwhile, in **(BLM+NIN)**, few cells with strong positive BCL-2 immune reaction were seen in the inter-alveolar septa (Fig9. 1D). Also, sections of **(BLM+MP+NIN)** showed few cells with strong positive immune reaction for BCL-2, in inter alveolar septa (Fig9. 1E).

The effect of nintedanib and methylprednisolone either alone or in combination on the mean thickness of the interalveolar septa in (µm) in lug tissue in a mice model of corticosteroid resistance pulmonary fibrosis induced by bleomycin after day 7 post treatments:

Bleomycin group and Bleomycin group treated with methylprednisolone showed significant ($P<0.0001$) increase in the interalveolar septa thickness as compared to the treated group with nintedanib alone (3.62±0.18 µm) and to the group of mice treated with nintedanib and methylprednisolone (3.68±0.14µm). Interestingly, there was non-significant ($P=0.95$) difference between treated mice with nintedanib alone and the group of mice treated with nintedanib and methylprednisolone as showed in table 1.

The effect of nintedanib and methylprednisolone either alone or in combination on the mean alveolar space surface area (μm^2) in lug tissue in a mice model of corticosteroid resistance pulmonary fibrosis

induced by bleomycin after day 7 post- treatments:

The bleomycin group and Bleomycin group treated with methylprednisolone showed significant ($P<0.0001$) decrease in the mean alveolar space surface area as compared to the treated group with nintedanib alone and to the group of mice treated with nintedanib and methylprednisolone. Interestingly, there was significant increase ($P<0.01$) in the mean alveolar space surface area in the group of mice treated with nintedanib and methylprednisolone compared to the group of bleomycin treated with nintedanib alone as showed in table 1.

The effect of nintedanib and methylprednisolone either alone or in combination on the scoring of lung parenchymal degeneration and the scoring of air way inflammation in lug tissue in a mice model of corticosteroid resistance pulmonary fibrosis induced by bleomycin after day 7 post-treatments:

Table1 showed non-significant ($P=0.17$) difference between bleomycin group and bleomycin treated mice with methylprednisolone. Moreover, the treated group with nintedanib alone and the group of mice treated with nintedanib methylpredinsolone showed significant ($P=0.0001$, $P<0.0001$; respectively) decrease in the scoring of lung parenchymal degeneration as compared to the group of bleomycin treated with methylprednisolone. No significant difference between treated mice with nintedanib alone and to the group of mice treated with nintedanib and methylprednisolone.

The effect of nintedanib and methylprednisolone either alone or in combination on the scoring of air way inflammation in lug tissue in a mice model of corticosteroid resistance pulmonary fibrosis induced by bleomycin after day 7 post- treatments:

In table 1, the bleomycin treated mice with methylprednisolone showed highly significant ($P<0.0001$, $P<0.0001$; respectively) increase in the airway inflammation scoring as compared to the treated group with nintedanib alone and to the group of mice treated with nintedanib and methylprednisolone. No significant ($P=0.17$) difference between treated mice with nintedanib alone and to the group of mice treated with nintedanib and methylprednisolone.

Table 1: Showed the effect of nintedanib and methylprednisolone either alone or in combination on the mean thickness of the interalveolar septa in (µm), the mean alveolar space surface area (μm^2), the scoring of lung parenchymal degeneration and the scoring of air way inflammation in lug tissue in a mice model of corticosteroid resistance pulmonary fibrosis induced by bleomycin after day 7:

Mice groups N=6	The mean thickness of the interalveolar septa in (µm) Mean ± SEM	The mean alveolar space surface area (μm^2) Mean ± SEM	Scoring of Lung parenchymal degeneration Mean± SEM	Scoring of Airway inflammation Mean± SEM
Control group	3.36±0.24	782.83±17.29	000	000
BLM group	30.87±1.38 *	343.66±9.43 *	2.50±0.22	2.16±0.31
BLM+MP group	37.77±1.29 *, #	226.22±17.98 *, #	3.66±0.22	3.00±0.00 #
BLM+NIN group	3.62±0.18 #, $	533.61±19.25 #, $	1.50±0.33#, $	1.33±0.21#, $
BLM+ (MP+NIN) group	3.68±0.14 #, $	601.94± 26.39 #, $, @	1.00±0.36 #, $	1.00±0.26 #, $

Data Values were mean ± standard error of mean (SEM); N = number of animals. BLM; bleomycin, MP; methylprednisolone, NIN; nintedanib. (%) = mean percentage change compared to control group. ANOVA one-way, accompanied by a multiple comparison test by Tukey. * Control group compared to other groups. # BLM group compared to treatments group. $ BLM+MP group compared to BLM+NIN and BLM+(MP+NINI). @ BLM+NIN compared to BLM+ (MP + NIN) group.

The effect of nintedanib and methylprednisolone either alone or in combination on the mean area percentage of positive BCL2 cells and the grading system of the intensity of immunohistochemical staining in lung tissues in a mice model of corticosteroid resistance pulmonary fibrosis induced by bleomycin after day 7 post treatments:

The expression of BCL-2 was significantly upregulated in bronchiolar cells, alveolar epithelial cells, interstial myofibroblasts and inflammatory cells after bleomycin instillation as compared to the bleomycin-treated mice with nintedanib alone and bleomycin-treated mice with methylprednisolone and nintedanib. Interestingly, the expression of BCL-2 was significantly ($P<0.0001$) upregulated in

inflammatory cells in bleomycin-treated mice with nintedanib alone as compared to bleomycin-treated mice with methylprednisolone and nintedanib. No significant (P>0.05) difference in the expression of BCL-2 in the bronchiolar epithelium, alveolar epithelial cells, and interstial myofibroblasts in bleomycin-treated mice with nintedanib alone as compared to bleomycin-treated mice with methylprednisolone and nintedanib as showed in table 2.

Table 2: showed the effect of nintedanib and methylprednisolone either alone or in combination on the expression of BCL-2 cells in lung tissues in a mice model of corticosteroid resistance pulmonary fibrosis induced by bleomycin:

The mean area percentage of positive BCL2 cells (Mean ± SEM)					
Groups (N=6)		Bronchiolar cells	Alveolar epithelial cells	Interstitial myofibroblasts	Inflammatory cells
Control group	F	2.86± 0.23	3.28±0.06	1.51±0.18	1.79±0.24
	G	0	0	0	0
BLM group	F	68.14±2.63*	27.13±0.31 *	81.31±2.06 *	77.69±2.08 *
	G	3	2	3	3
BLM+MP group	F	73.00±1.60 *, #	27.09±0.22 *	80.67±1.24 *	77.45±0.82*
	G	3	2	3	3
BLM+NIN group	F	2.70±0.25 #, $	10.02±0.01#, $	12.73±0.22#, $	18.80±1.47#,$
	G	0	1	2	2
BLM+(MP+NIN) group	F	1.71±0.21 #, $	10.33±0.18 #, $	11.86±0.17#, $	12.64±0.54 #, $, @
	G	0	1	2	2

F: Frequency expressed as percentage of immunoreactive cells; G: Staining grade expressed as: Grade 0: No staining or less than 10% positive cells; Grade 1: 10% positive cells, Grade 2: 10% - 50% positive cells, Grade 3: More than 50% positive cells. Data Values were mean ± standard error of mean (SEM); N = number of animals. BLM; bleomycin, MP; methylprednisolone, NIN; nintedanib. (%) = mean percentage change compared to control group. ANOVA one-way, accompanied by a multiple comparison test by Tukey. * Control group compared to other groups. # BLM group compared to treatments group. $ BLM+MP group compared to BLM+NIN and BLM+(MP+NINI). @ BLM+NIN compared to BLM+ (MP + NIN) group.

The effect of nintedanib and methylprednisolone either alone or in combination on the area percentage of collagen fibers in lung tissue in a mice model of corticosteroid resistance pulmonary fibrosis induced by bleomycin after day 28 post treatments:

The bleomycin group and bleomycin group treated with methylprednisolone showed significant increase in the mean area percentage of collagen fibers as compared to the treated group with nintedanib alone and to the group of mice treated with nintedanib and methylprednisolone. Interestingly, there was significant increase between treated mice with nintedanib alone as compared to the group of mice treated with nintedanib and methylprednisolone as showed in table 3.

The effect of nintedanib and methylprednisolone either alone or in combination on the mean of the subepithelial connective tissue volume density (VVsub) (mm) in lung tissue in a mice model of corticosteroid resistance pulmonary fibrosis induced by bleomycin after day 28 post treatments:

The bleomycin group and bleomycin group treated with methylprednisolone showed significant increase in the mean subepithelial connective tissue volume density (VVsub) as compared to the treated group with nintedanib alone and to the group of mice treated with nintedanib and methylprednisolone. Interestingly, there was significant increase between treated mice with nintedanib alone as compared to the group of mice treated with nintedanib and methylprednisolone as showed in table 3.

Table 3: showed the effect of nintedanib and methylprednisolone either alone or in combination on the area percentage of collagen fibers and the mean of the subepithelial connective tissue volume density (VVsub) (mm) in lung tissue in a mice model of corticosteroid resistance pulmonary fibrosis induced by bleomycin:

Groups (N=6)	The area percentage of collagen fibers Mean ± SEM	The mean of the subepithelial connective tissue volume density (VVsub) (mm) Mean± SEM
Control group	4.47±0.12	0.01± 0.001
BLM group	31.82± 0.88*	0.09± 0.002*
BLM+MP group	35.56± 0.34 *, #	0.0920± 0.002*
BLM+NIN group	7.99± 0.27 #, $	0.04±0.002 #, $
BLM+ (MP+NIN) group	5.18± 0.04 #, $, @	0.02±0.002#, $, @

Data Values were mean ± standard error of mean (SEM); N = number of animals. BLM; bleomycin, MP; methylprednisolone, NIN; nintedanib. (%) = mean percentage change compared to control group. ANOVA one-way, accompanied by a multiple comparison test by Tukey. * Control group compared to other groups. # BLM group compared to treatments group. $ BLM+MP group compared to BLM+NIN and BLM+(MP+NINI). @ BLM+NIN compared to BLM+ (MP + NIN) group.

Discussion

In this study assessment of potential therapy of nintedanib either alone or combined with methylprednisolone on bleomycin induced corticosteroid resistance pulmonary fibrosis in mice was done. In this model many inflammatory mediators and cytokines are released as IL-2, IL-4, IFN-y and TNF-α. The interleukin-2 (IL-2) is important in the development of fibrosis by supported cell mediated immunity and in general promote tissue restoration(Keane, 2008). In present study, there was a significant reduction in the level of IL-2 by 68.5%in lung tissue in the bleomycin group treated with MP compared to bleomycin group in addition there was more significant reduction in the IL-2 content by 84% in the lung tissue in nintedanib alone and in combination with methylprednisolone compared to bleomycin group on day 7 post treatment. Moreover, the interleukin − 4 (IL-4) is important in inflammation and fibrosis by more involved with antibody-mediated immunity, and tend to promote fibroblast activation, matrix development and,

therefore, fibrosis(Keane, 2008). In present study, the bleomycin treated with MP significantly decreased the level of IL-4 in lung tissue by 65.2% compared to bleomycin in addition there was more significant reduction in the level of IL-4 in lung tissue in the group of bleomycin treated with NIN and the group of bleomycin treated with MP + NIN by 74.7% and 72.7% respectively compared to bleomycin group. Also, IF-y is important in the development of fibrosis by supported cell mediated immunity and in general promote tissue restoration(Keane, 2008). The BLM + MP group significantly decreased the level of INF-y by 58.2% in lung tissue compared to BLM group in addition there was more significant reduction in the level of INF-y in lung tissue in BLM + NIN & BLM + MP + NIN groups by 65.6% & 67.1% respectively compared to BLM group. Additionally, activation of alveolar macrophages purified from the lung of mice instilled with bleomycin release pro-inflammatory mediators such as TNF-α as well as MIP-2, responsible for the persistence of inflammation and the development of fibrosis(Barbarin et al., 2005). In current study, the BLM + MP group significantly decreased the level of TNF-α by 67.15% in lung tissue compared to BLM group in addition there was more significant reduction in the level of TNF-α in lung tissue in BLM + NIN & BLM + MP + NIN by 74.7% & 77.1% respectively compared to BLM group. In Japanese article found that the level of cytokines in the lung tissue were studied with the reverse-transcriptase polymerase chain reaction. Levels of promotor cytokines, such as IL-2, IL-4, INF-y and TNFα were significantly higher in lung tissue in the bleomycin group. The expression of these cytokines in the glucocorticoid group was low, especially the peak value, but the expression of IL-4 was high in the bleomycin group and was not reduced in the glucocorticoid group(Hosoya, 1997). But, they found that significantly decreased in inflammatory cytokines after nintedanib treatment because it is act as anti-inflammatory effect as in study (Kim et al., 2018). Also, Ubieta, Thomas et al found that nintedanib inhibited the release of cytokines such as IFN-γ, IL-2, IL-4, IL-5, IL-10, IL-12p70 and IL-13, which may cause a clinical benefit in pulmonary fibrosis in interstitial lung diseases. Also, IL-2 has able to bind to lung fibroblasts, and proliferation of fibroblast induced by IL-2. IL-4 act directly on lung fibroblast to induce a fibro- genic response. However, IFN-γ, which is also reduced by nintedanib, exhibits potent antifibrotic activity by inhibiting synthesis of collagen in fibroblasts (Ubieta et al., 2021). Moreover, the oxidative stress is defined as extra production of reactive oxygen species (ROS) or decreases in antioxidants. The oxidative stress plays a role in lung fibrosis. Malondialdehyde (MDA) is one of the end products of polyunsaturated fatty acids peroxidation in the cells. An increase in free radicals causes overproduction of MDA in lung injury. Glutathione is a low molecular weight antioxidant found in normal lungs, is reduced in the epithelial lining fluid and fibrotic foci in pulmonary fibrosis(Cheresh et al., 2013). In current study, there was a little reduction in the level of MDA by 46.77 in lung tissue in BLM + MP group compared to bleomycin group in addition there was more significant reduction in the level of MDA by 77.4% & 80%in lung tissue in groups of BLM + NIN& BLM + MP + NIN compared to bleomycin group and there was a significant reduction in level of MDA in group of BLM + NIN& BLM + MP + NIN compared to BLM + MP group. Also, there was a significant increase in level of GSH by 540% in lung tissue in BLM + MP group compared to bleomycin group in addition there was a significant increase in level of GSH by 759.75% & 789.64% in lung tissue in BLM + NIN& BLM + MP + NIN groups compared to bleomycin group. And there was a significant increase in level of GSH in BLM + NIN& BLM + MP + NIN groups compared to BLM + MP group. Also, the effect of nintedanib and methylprednisolone in combination in level of GSH was much

better than the effect of nintedanib alone. The present study is agree with they found that the production of MDA in lung tissues was increased and GSH production in lung tissues was decreased in after bleomycin treatment (Liu et al., 2017b). Furthermore, TGFβ is play important role in fibrosis by stimulating fibroblast proliferation and the synthesis of extracellular matrix proteins, recruiting inflammatory cells through MCP-1 (CCL2) and inhibiting T-cell responses with contribute to healing of wound and fibrosis and Hydroxyproline also plays important role in the collagen synthesis and stability. (Wilson and Wynn, 2009). In present study, there was a significant decrease in the level of TGF-β in BLM + MP group by58.4 % compared to bleomycin group, in addition there was more significant reduction in content of TGF-β in lung tissue in BLM + NIN& BLM + MP + NIN groups by 66% compared to bleomycin group after 28 days post treatment. Also, there was a significant decrease in the level of hydroxyproline in BLM + MP group by 77.2% compared to bleomycin group, in addition there was more significant reduction in content of hydroxyproline in lung tissue in BLM + NIN& BLM + MP + NIN groups by 88% compared to bleomycin group after 28 days post treatment. Khalil et al found that the corticosteroid therapy administered in the advanced stages of the disease would likely not suppress the TGF-b production by alveolar macrophages. The relative resistance to corticosteroid therapy in pulmonary inflammatory and fibrotic responses seen in many human lung diseases may be caused by the corticosteroid insensitivity of TGF-b production by alveolar macrophages(Khalil et al., 1993). The water content in lung tissue after 28 days post treatment, it was a significant reduce in water content in bleomycin group with nintedanib either alone or in combination with methypredisolone compared to bleomycin group in addition there was no significant difference between bleomycin group and bleomycin group treated with MP. Our finding agree with They found that dexamethasone treatment did not prevent bleomycin-induced edema (Aubin Vega et al., 2019). Similarly, to dexamethasone, another corticosteroid did not elicit any beneficial effect on lung edema in bleomycin mice. Also, our finding agree with pervious study found the effect of Nintedanib in a rat model of lung fibrosis induced by bleomycin and they showed a significant decrease in water content compared to bleomycin group(Pittelli et al., 2017). Our study's histological findings showed that methylprednisolone was unable to enhance the histological outcomes of the bleomycin model of lung fibrosis after 7 and 28 days in the current research. This was in line with prior research by (Dik et al., 2003, Bahtouee et al., 2018, Aubin Vega et al., 2019). MP therapy increased the expansion of alveolar airspaces and the decrease in lung compliance, according to(Langenbach et al., 2007). Also, Aubin Vega et al. investigated the effect of corticosteroids on the bleomycin outcomes during the acute exudative phase after 3 and 7 days. They found that exposure to bleomycin and dexamethasone exhibited severe injury scores, alveolar damage at day 3 and at day 7. They stated that dexamethasone failed to reduce inflammatory cell infiltration and alveolar epithelial injury induced by bleomycin. Dexamethasone affected the expression of β3- and β6-integrins, key proteins of alveolar repair(Aubin Vega et al., 2019). Previous research has demonstrated that long-term corticosteroid treatment, either before or at the same time as bleomycin treatment, reduced the development of lung fibrosis in rats(Phan et al., 1981, Cross et al., 1985, Shaker and Sourour, 2011). Moreover, in the present study, methylprednisolone does not reverse the bleomycin-repair impairment, but it further worsened the bronchiolar epithelial condition. The epithelial lining of the bronchiolar passages showed marked disorganization and degeneration in which their epithelial lining exhibited vacuolation with eukaryotic

nuclei. Their lumen appeared obliterated by detached epithelial cells. Dexamethasone has been found to have a negative influence on repair processes in bronchiolar epithelial cells, which is consistent with our findings (Liu et al., 2013, Kadmiel et al., 2016). According to these findings, bleomycin-induced pulmonary fibrosis is resistant to suppression by concurrent MP therapy. In current study, we used the QPCR for expression of integrins. Integrins are membrane-bound proteins that play an important role in maintenance and remodeling of ECM by transmitting signals from the ECM to control cell function. In the case of the fibroblast, integrin expression can influence the expression of intracellular structural or contractile proteins, such as alpha-smooth muscle actin (αSMA), and thus the myofibroblast phenotype, as well as extracellular structural proteins, such as collagen(Merna et al., 2015). In present study, negative effect of methylprednisolone alone compared to control group, but the effect of nintedanib alone and in combination with methylprednisolone was little increased in β3& β6 integrins gene in lug tissue compared to bleomycin group. We discovered that nintedanib reduced BLM-induced alveolar inflammation and pulmonary fibrosis. In comparison to the BLM group, the mice in the nintedanib-treated and nintedanib and MP groups had reduced inflammatory cell infiltration and collagen deposition. This came in accordance with previous study(Wollin et al., 2013, Rangarajan et al., 2016, Redente et al., 2018, Chen et al., 2020). Chen et al. looked into the function of nintedanib in bleomycin-induced pulmonary fibrosis, comparing lung sections from pulmonary fibrosis mice who received nintedanib by oral gavage with those from mice with pulmonary fibrosis who did not. They discovered lung inflammation and fibrosis seven days after bleomycin-induced pulmonary fibrosis, which were substantially decreased by nintedanib therapy. They also discovered that animals given nintedanib had considerably lower lung damage scores, as well as reduced pulmonary fibrosis as measured by Masson's trichrome staining and the Ashcroft score seven days following bleomycin administration. Moreover, Wollin *et al.* investigated nintedanib at 30 mg/kg or 60 mg/kg as a preventive treatment (from day 0 to day 14) and as a therapeutic treatment (from day 7 to 21) in a mouse model of lung inflammation and fibrosis by a single intratracheal administration of bleomycin. They found that therapeutic therapy at 60 mg/kg had similar inhibitory effects as preventative treatment, while the effect magnitude was lower at 30 mg/kg. They found that nintedanib successfully decreased pulmonary inflammation and fibrosis in mice whether given as a preventative or therapeutic therapy. Nintedanib's anti-inflammatory and anti-fibrotic properties may have an influence on the progression of fibrotic lung disorders such IPF(Wollin et al., 2013). Apoptosis is a form of cell death that plays a critical function in the maintenance of cellular homeostasis. The Bcl-2 family of proteins is one of the most essential regulators of the apoptosis process (Dewson and Kluck, 2010). Bcl-2 protein is an intracellular membrane-associated protein that inhibits cell death when overexpressed (Nemec and Khaled, 2008, Youle and Strasser, 2008, Dewson, 2011). Bcl-2 family members appear to play a critical role in the pathogenesis of inflammation, apoptosis, and fibrosis produced by different causes in interstitial lung disorders, according to an increasing body of data (Safaeian et al., 2014). In the current study, in group II (BLM group) and group III (BLM group treated with MP) there was upregulation of positive immune reaction in the inter-alveolar septa and the interstitium of the lung. While few positive immune reactions were seen in the epithelium lining the bronchiole lumen. High expression of the anti-apoptotic gene Bcl-2 and low expression of the pro-apoptotic gene Bax prevented apoptosis in lung fibroblasts following bleomycin instillation, which is a major characteristic of

chronic fibrotic illnesses, according to our findings, which are similar with previous research(Safaeian et al., 2009, Aguilar et al., 2009, Zhou et al., 2013, Hu and Zhu, 2020). Furthermore, the current findings were consistent with those of Safaeian et al., who discovered BCL-2 immunoreactivity in a variety of cells, including bronchiolar epithelial cells and lymphocytes, macrophages, neutrophils, alveolar epithelial cells, and myofibroblasts, and found that their interactions are linked to the development of interstitial fibrosis after bleomycin instillation(Safaeian et al., 2008). Predescu et al., on the other hand, detected no alterations in Bcl-2 and Bcl-xL during Fas-mediated apoptosis in primary lung fibroblasts(Predescu et al., 2017). The extracellular matrix-producing myofibroblasts that collect in fibrotic lung lesions gain resistance to apoptosis in pulmonary fibrosis (Thannickal and Horowitz, 2006, Potter-Perigo et al., 2010). Nintedanib has been found to inhibit fibroblast proliferation, migration, and transformation, although its effects on apoptosis have yet to be investigated(Wollin et al., 2015). In the present study, the treatment with nintedanib and the combined treatment of methylprednisolone and nintedanib were more effective in a model of pulmonary fibrosis. There was an apparent decrease of the positive immune reaction for BCL-2 in inter alveolar septa with negative BCL-2 of bronchiolar epithelium. The present results were similar to the findings of studies by (Milara et al., 2018). Milara et al. discovered that JAK2 and STAT3 are activated in IPF in a rat model of bleomycin-induced lung fibrosis, and that their dual inhibition could be an appealing strategy for inhibiting fibroblast migration, preventing increases in fibroblast senescence and Bcl-2 expression, and improving impaired autophagy. Rangarajan et al. discovered that nintedanib enhances the apoptotic clearance of fibrocytes and lung-resident myofibroblasts, slowing the development of TGF-induced pulmonary fibrosis. In fibroblasts isolated from IPF lungs, nintedanib was reported to activate autophagy(Rangarajan et al., 2016). Furthermore, nintedanib can prevent fibrocyte migration, lowering the amount of fibrocytes in the lungs during bleomycin-induced pulmonary fibrosis(Sato et al., 2017b). **limitations of study** include small size of samples per group, the analysis was done just at day 7 & day 28.

Conclusion

Altogether, our data indicates that the nintedanib overcame on the corticosteroid resistance pulmonary fibrosis induced by bleomycin because the bleomycin group treated with nintedanib alone and bleomycin group treated with methylprednisolone and nintedanib were able to improve the alveolar damage and decrease the collagen deposition with decrease edema in the lung and reduce the inflammatory cells.

Declarations

Ethical Approval:

This study has been approved by the Faculty of Pharmacy, King Abdulaziz University Research Ethics Committee.

Competing interests:

The authors declare that they have no competing interests.

Funding:

The main author's money.

Authors' contribution:

Doha O Alghamdi wrote the manuscript and provided data for Tables & graphs and all statistical analyses, Hala S Abdel Kawy conducted the histological analysis with review all data and statistical analyses, and Zuhair A Damanhouri reviewed all methods work and gave comments. All authors reviewed the final manuscript.

Corresponding author

Correspondence to Doha Alghamdi

Email: dohaalghamdi93@gmail.com

Phone: 00966506264627

Jeddah, K.S.A

Acknowledgement:

I would like to express my special thanks of gratitude to Prof. Dr. Hala Salah Abdel Kawy, Professor of Pharmacology Faculty of Medicine, King Abdulaziz University for their able guidance and support in completing the research. I extend my special thanks to the staff of pharmacology department, medicine college, King Abdul-Aziz University, Jeddah, KSA. I am thankful for the help provided by my parents, husband, my daughter, sister, and brothers.

Abbreviations

AEC	alveolar epithelial cell
AP-1	Anti-intestinal alkaline phosphatase antibody
a-SMA	Alpha-smooth muscle actin
BLM	Bleomycin
C-Abl	c-Abelson tyrosine kinase
COPD	Chronic obstructive pulmonary disease
COVID-19	Coronavirus-19
ECM	Extracellular matrix
ELIZA	enzyme-linked immunosorbent assay
EMT	Epithelial–mesenchymal Transition
FGFR	Fibroblast growth factor receptor
GSH	Glutathione
GR	Glucocorticoid receptor
HDAC2	Histone deacetylase 2
H&E	Hematoxylin and eosin stain
H2RA	Histamine 2 receptor agonist
IL	Interleukins
ILD	interstitial lung disease
INF	Interferon
IPF	Idiopathic pulmonary fibrosis
MDA	Malondialdehyde
MIF	Macrophage migration inhibitory factor
NIN	Nintedanib
PDGF	Platelet-derived growth factor
PF	Pulmonary fibrosis
ROS	Reactive Oxygen Species

RT-Q PCR	Real time Quantitative polymerase chain reaction
SARS-COV2	Severe acute respiratory syndrome coronavirus 2
SEM	Standard error of mean
TB	Tuberculosis
TGF	Transforming growth factor
TNF	Tumor necrosis factor
VEGF	Vascular endothelial growth factor
W/D	Wet/dry

References

ACHARYA N, MISHRA SHARMA,SK, DHIR DDHOORIA,S, V. & JAIN S. Efficacy and safety of pirfenidone in systemic sclerosis-related interstitial lung disease—a randomised controlled trial. Rheumatol Int. 2020;40:703–10.

ADAMSON I. Pulmonary toxicity of bleomycin. Environmental health perspectives. 1976;16:119–25.

AGUILAR S, SCOTTON CJ, MCNULTY K, NYE E, STAMP G, LAURENT G, BONNET D, JANES SM. Bone marrow stem cells expressing keratinocyte growth factor via an inducible lentivirus protects against bleomycin-induced pulmonary fibrosis. PloS one. 2009;4:e8013.

AHMED BS, ANWAR NM. Immuno-histochemical study of the expression of Bcl-2 in the Leydig's interstitial cells and primary spermatocyte cells of adult male rabbit under the effect of oral Gossypol intake. The Egyptian Journal of Hospital Medicine. 2004;14:34–44.

AONO Y, NISHIOKA Y, INAYAMA M, UGAI M, UEHARA KISHI,J, H., IZUMI, K. & SONE S. Imatinib as a novel antifibrotic agent in bleomycin-induced pulmonary fibrosis in mice. Am J Respir Crit Care Med. 2005;171:1279–85.

AUBIN VEGA M, PASCARIU CHUPIN,C, DAGENAIS MPRIVÉ,A, BERTHIAUME A, Y. & BROCHIERO E. Dexamethasone fails to improve bleomycin-induced acute lung injury in mice. Physiological reports. 2019;7:e14253.

BAHTOUEE M, MOVAHED FATEMIKIA,H, ESMAILI A, HASSAN A, ZAREI Y, M. & SEYEDIAN R. A comparative analysis of saffron and methylprednisolone on bleomycin-induced pulmonary fibrosis in rats. Iranian Journal of Toxicology. 2018;12:9–13.

BARBARIN V, NIHOUL A, MISSON P, ARRAS M, DELOS M, LECLERCQ I, LISON D, HUAUX F. The role of pro- and anti-inflammatory responses in silica-induced lung fibrosis. Respiratory research. 2005;6:1–13.

BARNES PJ. Mechanisms and resistance in glucocorticoid control of inflammation. J Steroid Biochem Mol Biol. 2010;120:76–85.

BI J, DAI J, KOIVISTO L, LARJAVA M, BI L, HÄKKINEN L, LARJAVA H. Inflammasome and cytokine expression profiling in experimental periodontitis in the integrin β6 null mouse. Cytokine. 2019;114:135–42.

BI J, KOIVISTO L, OWEN G, HUANG P, WANG Z, SHEN Y, BI L, HAAPASALO ROKKA,A, M. & HEINO J. Epithelial microvesicles promote an inflammatory phenotype in fibroblasts. Journal of dental research. 2016;95:680–8.

BOGATKEVICH GS, NIETERT PJ, SILVER RM, HIGHLAND KB. Rationale for anticoagulant therapy of pulmonary fibrosis. Am J Respir Crit Care Med. 2014;189:362–3.

CALAWAY AC, FOSTER RS, ALBANY ADRA,NMASTERSON,TA, C., HANNA, N. H., EINHORN, L. H. & CARY C. Risk of bleomycin-related pulmonary toxicities and operative morbidity after postchemotherapy retroperitoneal lymph node dissection in patients with good-risk germ cell tumors. ASCO; 2018.

CHAMBERS R. Abnormal wound healing responses in pulmonary fibrosis: focus on coagulation signalling. European Respiratory Review. 2008;17:130–7.

CHAUDHARY NI, SCHNAPP A, PARK JE. Pharmacologic differentiation of inflammation and fibrosis in the rat bleomycin model. Am J Respir Crit Care Med. 2006;173:769–76.

CHEN W-C, CHEN N-J, CHEN CHEN,H-P,YU,W-K,SU,VY-F, H., WU, H.-H. & YANG K-Y. Nintedanib reduces neutrophil chemotaxis via activating GRK2 in bleomycin-induced pulmonary fibrosis. Int J Mol Sci. 2020;21:4735.

CHERESH P, KIM S-J, TULASIRAM S, KAMP DW. Oxidative stress and pulmonary fibrosis. Biochimica et Biophysica Acta (BBA)-Molecular Basis of Disease. 2013;1832:1028–40.

CLAUSSEN CA, LONG EC. Nucleic acid recognition by metal complexes of bleomycin. Chemical reviews. 1999;99:2797–816.

CROSS CE, WARREN D, WILSON GERRIETS,JE, HALLIWELL DW, B. & LAST JA. Deferoxamine injection does not affect bleomycin-induced lung fibrosis in rats. J Lab Clin Med. 1985;106:428–32.

DANIELS CE, GABOR LASKY,JA,LIMPER,AH,MIERAS,K, E. & SCHROEDER DR. Imatinib treatment for idiopathic pulmonary fibrosis: randomized placebo-controlled trial results. Am J Respir Crit Care Med. 2010;181:604–10.

DELLA LATTA V, CECCHETTINI A, DEL RY S, MORALES MA. Bleomycin in the setting of lung fibrosis induction: From biological mechanisms to counteractions. Pharmacological research. 2015;97:122–30.

DEWSON G. 2011. Interplay of Bcl-2 proteins decides the life or death fate. *The Open Cell Signaling Journal*, 3.

DEWSON G, KLUCK RM. Bcl-2 family-regulated apoptosis in health and disease. Cell Health Cytoskeleton. 2010;2:9–22.

DIK W, MCANULTY R, VERSNEL M, NABER B, LAURENT ZIMMERMANN,L, G. & MUTSAERS S. Short course dexamethasone treatment following injury inhibits bleomycin induced fibrosis in rats. Thorax. 2003;58:765–71.

FARRAND E, VITTINGHOFF E, LEY B, BUTTE, A. J. & COLLARD HR. Corticosteroid use is not associated with improved outcomes in acute exacerbation of IPF. Respirology. 2020;25:629–35.

FAVERIO P, DE GIACOMI F, SARDELLA L, FIORENTINO G, CARONE M, SALERNO F, ROGLIANI ORA,J, PELLEGRINO P, G. & PAPA GFS. Management of acute respiratory failure in interstitial lung diseases: overview and clinical insights. BMC pulmonary medicine. 2018;18:1–13.

FLAHERTY KR, TOEWS,GB,LYNCH III, JP, KAZEROONI, EA,GROSS,BH,STRAWDERMAN III, RL, HARIHARAN, FLINT K, A. & MARTINEZ FJ. Steroids in idiopathic pulmonary fibrosis: a prospective assessment of adverse reactions, response to therapy, and survival. Am J Med. 2001;110:278–82.

FLAHERTY KR, COTTIN WELLS,AU, DEVARAJ V, WALSH A, INOUE SL, RICHELDI Y, KOLB L, TETZLAFF M, K. & STOWASSER S. Nintedanib in progressive fibrosing interstitial lung diseases. N Engl J Med. 2019;381:1718–27.

GAD E, SALAMA A, EL-SHAFIE M, ARAFA H, ABDELSALAM R, KHATTAB M. 2019. The Anti-fibrotic and Anti-inflammatory Potential of Bone Marrow–Derived Mesenchymal Stem Cells and Nintedanib in Bleomycin-Induced Lung Fibrosis in Rats. *Inflammation*, 1–12.

GALUPPO M, ESPOSITO E, MAZZON E, DI PAOLA R, PATERNITI I, IMPELLIZZERI D, CUZZOCREA S. MEK inhibition suppresses the development of lung fibrosis in the bleomycin model. Naunyn Schmiedebergs Arch Pharmacol. 2011;384:21–37.

GINZBURG VE. Chest pain, dyspnea, and cough. Canadian family physician Medecin de famille canadien. 2006;52:1060–0.

GREEN FH. Overview of pulmonary fibrosis. Chest. 2002;122:334S–339S.

GROSS TJ, HUNNINGHAKE GW. Idiopathic pulmonary fibrosis. N Engl J Med. 2001;345:517–25.

GRZESK G, WOZNIAK-WISNIEWSKA A. Bła zejewski. Int J Mol Sci. 2021;22:282.

HAGIWARA S-I, ISHII Y, KITAMURA S. Aerosolized administration of N-acetylcysteine attenuates lung fibrosis induced by bleomycin in mice. Am J Respir Crit Care Med. 2000;162:225–31.

HAY J, SHAHZEIDI S, LAURENT G. Mechanisms of bleomycin-induced lung damage. Arch Toxicol. 1991;65:81–94.

HERRERA J, HENKE, C. A. & BITTERMAN PB. Extracellular matrix as a driver of progressive fibrosis. J Clin Investig. 2018;128:45–53.

HOSOYA T. Steroid resistance and lung-tissue cytokines in experimental bleomycin-induced lung fibrosis. The Japanese journal of thoracic diseases. 1997;35:766–75.

HU X, HUANG X. Alleviation of inflammatory response of pulmonary fibrosis in acute respiratory distress syndrome by puerarin via transforming growth factor (TGF-β1). Medical science monitor: international medical journal of experimental clinical research. 2019;25:6523.

HU X, ZHU D. Rehmannia Radix Extract Relieves Bleomycin-Induced Pulmonary Fibrosis in Mice via Transforming Growth Factor β1 (TGF-β1). Medical Science Monitor: International Medical Journal of Experimental Clinical Research. 2020;26:e927240-1.

HUANG SH, CAO XJ, LIU W, SHI, X. Y. & WEI W. Inhibitory effect of melatonin on lung oxidative stress induced by respiratory syncytial virus infection in mice. Journal of pineal research. 2010;48:109–16.

ITO Y, TAZAKI G, KONDO Y, TAKAHASHI G, SAKAMAKI F. Therapeutic effect of nintedanib on acute exacerbation of interstitial lung diseases. Respiratory medicine case reports. 2019;26:317–20.

IZBICKI G, SEGEL M, CONNER CHRISTENSEN,T, M. & BREUER R. Time course of bleomycin-induced lung fibrosis. Int J Exp Pathol. 2002;83:111–9.

JENKINS RG, EICKELBERG MOORE,BB,CHAMBERS,RC, KÖNIGSHOFF O, KOLB M, LAURENT M, G. J., NANTHAKUMAR, C. B., OLMAN, M. A. & PARDO A. An official American Thoracic Society workshop report: use of animal models for the preclinical assessment of potential therapies for pulmonary fibrosis. Am J Respir Cell Mol Biol. 2017;56:667–79.

KADMIEL M, XU JANOSHAZI,A, X. & CIDLOWSKI JA. Glucocorticoid action in human corneal epithelial cells establishes roles for corticosteroids in wound healing and barrier function of the eye. Exp Eye Res. 2016;152:10–33.

KARIMI-SHAH BA, CHOWDHURY BA. Forced vital capacity in idiopathic pulmonary fibrosis–FDA review of pirfenidone and nintedanib. N Engl J Med. 2015;372:1189–91.

KASAM RK, REDDY, G. B., JEGGA, A. G. & MADALA SK. Dysregulation of mesenchymal cell survival pathways in severe fibrotic lung disease: The effect of nintedanib therapy. Front Pharmacol. 2019;10:532.

KEANE M. The role of chemokines and cytokines in lung fibrosis. European Respiratory Review. 2008;17:151–6.

KEATING GM. Nintedanib: a review of its use in patients with idiopathic pulmonary fibrosis. Drugs. 2015;75:1131–40.

KHALIL N, ZUO WHITMAN,C, DANIELPOUR L, D. & GREENBERG A. Regulation of alveolar macrophage transforming growth factor-beta secretion by corticosteroids in bleomycin-induced pulmonary inflammation in the rat. J Clin Investig. 1993;92:1812–8.

KIM H-Y, KIM M-S, KIM S-H, JOEN D, LEE K. 2018. Protective effects of nintedanib against polyhexamethylene guanidine phosphate-induced lung fibrosis in mice. *Molecules*, 23, 1974.

KIM JY, CHOENG HC, AHN C, CHO S-H. Early and late changes of MMP-2 and MMP-9 in bleomycin-induced pulmonary fibrosis. Yonsei Med J. 2009;50:68.

KIM MS, CHIN BAEK,AR,LEE,JH,JANG,AS, S. S. & PARK SW. IL-37 attenuates lung fibrosis by inducing autophagy and regulating TGF-β1 production in mice. J Immunol. 2019;203:2265–75.

KING CS, FREIHEIT E, ARYAL BROWN,AW,SHLOBIN,OA, KHANGOORA SAHMAD,K, VENUTO VFLAHERTY,KR, D. & NATHAN SD. Association Between Anticoagulation and Survival in Interstitial Lung Disease: An Analysis of the Pulmonary Fibrosis Foundation Patient Registry. Chest. 2021;159:1507–16.

KREUTER M, RENZONI WUYTS,W, KOSCHEL E, MAHER D, KOLB TM, WEYCKER M, SPAGNOLO D, P., KIRCHGAESSLER, K.-U. & HERTH FJ. Antacid therapy and disease outcomes in idiopathic pulmonary fibrosis: a pooled analysis. The Lancet Respiratory Medicine. 2016;4:381–9.

LANGENBACH SY, WHEATON BJ, FERNANDES DJ, JONES C, SUTHERLAND TE, WRAITH BC, HARRIS T, SCHULIGA MJ, MCLEAN C, STEWART AG. Resistance of fibrogenic responses to glucocorticoid and 2-methoxyestradiol in bleomycin-induced lung fibrosis in mice. Can J Physiol Pharmacol. 2007;85:727–38.

LI LF, LIN KAO,KC,LIU,YY, C. W., CHEN, N. H., LEE, C. S., WANG, C. W. & YANG CT. Nintedanib reduces ventilation-augmented bleomycin-induced epithelial–mesenchymal transition and lung fibrosis through suppression of the Src pathway. J Cell Mol Med. 2017;21:2937–49.

LIU J, ZHANG M, LUO NIU,C, DAI Z, LIU JWANG,L, E. & FU Z. Dexamethasone inhibits repair of human airway epithelial cells mediated by glucocorticoid-induced leucine zipper (GILZ). PLoS One. 2013;8:e60705.

LIU T, DE LOS SANTOS FG & PHAN, S. H. 2017a. The bleomycin model of pulmonary fibrosis. *Fibrosis.* Springer.

LIU Y, LU F, KANG L, WANG Z, WANG Y. Pirfenidone attenuates bleomycin-induced pulmonary fibrosis in mice by regulating Nrf2/Bach1 equilibrium. BMC pulmonary medicine. 2017b;17:1–11.

MASTRUZZO C, CRIMI N, VANCHERI C. Role of oxidative stress in pulmonary fibrosis. Monaldi archives for chest disease = Archivio Monaldi per le malattie del torace. 2002;57:173–6.

MATSUYAMA H, HASHIMOTO AMAYA,F, UENO S, BEPPU H, MIZUTA S, ISHIZAKA MSHIME,N, A. & HASHIMOTO S. Acute lung inflammation and ventilator-induced lung injury caused by ATP via the P2Y receptors: an experimental study. Respiratory research. 2008;9:1–13.

MAYR M, MEDRANO DUERRSCHMID,C, TAFFET G, WANG GE, ENTMAN Y, M. L. & HAUDEK SB. TNF/Ang-II synergy is obligate for fibroinflammatory pathology, but not for changes in cardiorenal function. Physiological reports. 2016;4:e12765.

MCCORMACK PL. Nintedanib: first global approval. Drugs. 2015;75:129–39.

MERNA N, KING FUNG,KM,WANG,JJ, CHRISTMAN CR,HANSEN,KC, K. L. & GEORGE SC. Differential β3 integrin expression regulates the response of human lung and cardiac fibroblasts to extracellular matrix and its components. Tissue Eng Part A. 2015;21:2195–205.

MEYER KC. Pulmonary fibrosis, part I: epidemiology, pathogenesis, and diagnosis. Expert Review of Respiratory Medicine. 2017;11:343–59.

MILARA J, HERNANDEZ G, BALLESTER B, ROGER MORELL,A, MONTERO I, MOLINA-MOLINA PESCRIVÁ,JLLORIS,JM, M. & MORCILLO E. The JAK2 pathway is activated in idiopathic pulmonary fibrosis. Respiratory research. 2018;19:1–12.

MOELLER A, ASK K, WARBURTON D, & KOLB GAULDIE,J, M. The bleomycin animal model: a useful tool to investigate treatment options for idiopathic pulmonary fibrosis? Int J Biochem Cell Biol. 2008;40:362–82.

MORALES V, ORTIZ-BUSTOS MARTÍN,A, SANZ J, R. & GARCÍA-MUÑOZ R. Effect of the dual incorporation of fullerene and polyethyleneimine moieties into SBA-15 materials as platforms for drug delivery. Journal of Materials Science. 2019;54:11635–53.

MOURATIS MA, AIDINIS V. Modeling pulmonary fibrosis with bleomycin. Curr Opin Pulm Med. 2011;17:355–61.

NEMEC KN, KHALED AR. Therapeutic modulation of apoptosis: targeting the BCL-2 family at the interface of the mitochondrial membrane. Yonsei Med J. 2008;49:689–97.

NETTELBLADT O, TENGBLAD A, HALLGREN R. High-dose corticosteroids during bleomycin-induced alveolitis in the rat do not suppress the accumulation of hyaluronan (hyaluronic acid) in lung tissue. Eur Respir J. 1990;3:421–8.

NETWORK IPFCR. Prednisone, azathioprine, and N-acetylcysteine for pulmonary fibrosis. N Engl J Med. 2012;366:1968–77.

OJO AS, WILLIAMS BALOGUN,SA, O. T. & OJO OS. 2020. Pulmonary fibrosis in COVID-19 survivors: predictive factors and risk reduction strategies. *Pulmonary medicine*, 2020.

PEIKERT T, DANIELS C, BEEBE T, MEYER K, RYU J, PHYSICIANS IL. D. N. O. T. A. C. O. C. 2008. Assessment of current practice in the diagnosis and therapy of idiopathic pulmonary fibrosis. *Respiratory medicine*, 102, 1342–1348.

PENG R, SRIDHAR S, TYAGI G, PHILLIPS JE, GARRIDO R, HARRIS P, BURNS L, RENTERIA L, WOODS J, CHEN L. Bleomycin induces molecular changes directly relevant to idiopathic pulmonary fibrosis: a model for “active” disease. PloS one. 2013;8:e59348.

PHAN SH, THRALL RS, WILLIAMS C. Bleomycin-induced pulmonary fibrosis: effects of steroid on lung collagen metabolism. Am Rev Respir Dis. 1981;124:428–34.

PITTELLI MG, PITOZZI V, CARUSO P, BONATTI M, AQUINO G, BIAGETTI M, QUAINI FRATI,CMANGIARACINA,C, F. & LAGRASTA C. Effect of Nintedanib in a rat model of lung fibrosis induced by single or double bleomycin administration. The European Respiratory Journal. 2017;50:PA2956.

POLOSUKHIN VV, DEGRYSE AL, NEWCOMB DC, JONES BR, WARE, L. B., LEE, J. W., LOYD, J. E., BLACKWELL, T. S. & LAWSON WE. 2012. Intratracheal bleomycin causes airway remodeling and airflow obstruction in mice. *Experimental lung research*, 38, 135–146.

POTTER-PERIGO S, EVANKO JOHNSON,PY, CHAN SP, WILKINSON CK,BRAUN,KR, ALTMAN TS, L. C. & WIGHT TN. Polyinosine-polycytidylic acid stimulates versican accumulation in the extracellular matrix promoting monocyte adhesion. Am J Respir Cell Mol Biol. 2010;43:109–20.

PREDESCU SA, ZHANG J, BARDITA C, PATEL M, GODBOLE, V. & PREDESCU DN. Mouse lung fibroblast resistance to Fas-mediated apoptosis is dependent on the baculoviral inhibitor of apoptosis protein 4 and the cellular FLICE-inhibitory protein. Frontiers in physiology. 2017;8:128.

RAGHU G, EGAN BEHR,JBROWN,KK, KAWUT JJ, FLAHERTY SM, K. R., MARTINEZ, F. J., NATHAN, S. D., WELLS, A. U. & COLLARD HR. Treatment of idiopathic pulmonary fibrosis with ambrisentan: a parallel, randomized trial. Ann Intern Med. 2013;158:641–9.

RAGHU G, ZHANG ROCHWERG,B, GARCIA Y, AZUMA CAC, CUNNINGHAM ABEHR,JBROZEK,JL,COLLARD,HR, W. & HOMMA S. An official ATS/ERS/JRS/ALAT clinical practice guideline: treatment of idiopathic pulmonary fibrosis. An update of the 2011 clinical practice guideline. Am J Respir Crit Care Med. 2015;192:e3–19.

RANGARAJAN S, KURUNDKAR KURUNDKAR,A, DING DBERNARD,KSANDERS,YY, ZHANG QANTONY,VB, ZMIJEWSKI J, J. & THANNICKAL VJ. Novel mechanisms for the antifibrotic action of nintedanib. Am J Respir Cell Mol Biol. 2016;54:51–9.

REDENTE EF, BLACK AGUILAR,MA, EDELMAN BP, WOLLIN BL,BAHADUR,AN,HUMPHRIES,SM,LYNCH,DA, L. & RICHES DW. Nintedanib reduces pulmonary fibrosis in a model of rheumatoid arthritis-associated interstitial lung disease. American Journal of Physiology-Lung Cellular Molecular Physiology. 2018;314:L998–1009.

REDENTE EF, LARA JACOBSEN,KM,SOLOMON,JJ, HENSON AR,FAUBEL,SKEITH,RC, P. M., DOWNEY, G. P. & RICHES DW. Age and sex dimorphisms contribute to the severity of bleomycin-induced lung injury and fibrosis. American Journal of Physiology-Lung Cellular Molecular Physiology. 2011;301:L510–8.

REINERT T, NUNES BALDOTTO,CSDR, F. A. P. & SCHELIGA, A. A. D. S. 2013. Bleomycin-induced lung injury. *Journal of Cancer Research*, 2013.

REN Y, ZHAO J, SHI Y, CHEN C, CHEN X, LV C. Simple determination of L-hydroxyproline in idiopathic pulmonary fibrosis lung tissues of rats using non-extractive high-performance liquid chromatography coupled with fluorescence detection after pre-column derivatization with novel synthetic 9-acetylimidazol-carbazole. J Pharm Biomed Anal. 2017;142:1–6.

RICHELDI L, DU BOIS RM, RAGHU G, AZUMA A, BROWN, K. K., COSTABEL, U., COTTIN, V., FLAHERTY, K. R., HANSELL, D. M. & INOUE Y. Efficacy and safety of nintedanib in idiopathic pulmonary fibrosis. N Engl J Med. 2014;370:2071–82.

ROSSI A, LATIANO TP, PARENTE P, CHIARAZZO C, LIMOSANI F, DI MAGGIO G, MAIELLO E. The potential role of nintedanib in treating colorectal cancer. Expert opinion on pharmacotherapy. 2017;18:1153–62.

ROTH GJ, BINDER R, COLBATZKY F, SCHLENKER-HERCEG DALLINGER,C, R., HILBERG, F., WOLLIN, S.-L. & KAISER R. Nintedanib: from discovery to the clinic. Journal of medicinal chemistry. 2015;58:1053–63.

SAFAEIAN L, ABED A, VASEGHI G. The role of Bcl-2 family proteins in pulmonary fibrosis. Eur J Pharmacol. 2014;741:281–9.

SAFAEIAN L, JAFARIAN A, RABANI M, TORABINIA MIRMOHAMMAD,SH, N. & ALAVI S. 2009. The effect of AT1 receptor blockade on bax and bcl-2 expression in bleomycin-induced pulmonary fibrosis.

SAFAEIAN L, RABBANI JAFARIAN,A, SADEGHI M, TORABINIA H, N. & ALAVI S. The role of strain variation in BAX and BCL-2 expression in murine bleomycin-induced pulmonary fibrosis. Pak J Biol Sci. 2008;11:2606.

SARAIVA GN, MEDEIROS ROSÁRIO,NFD, LEITE T, ANDRADE PECLACERDA,GDS, DE TGD, AZEREDO EL, ANCUTA P, ALMEIDA, J. R. & XAVIER AR. 2018. Restoring inflammatory mediator balance after sofosbuvir-induced viral clearance in patients with chronic hepatitis C. *Mediators of inflammation*, 2018.

SATO S, SHINOHARA S, HAYASHI S, MORIZUMI S, ABE S, OKAZAKI H, CHEN Y, GOTO H, AONO, Y. & OGAWA H. Anti-fibrotic efficacy of nintedanib in pulmonary fibrosis via the inhibition of fibrocyte activity. Respiratory research. 2017a;18:172.

SATO S, SHINOHARA S, HAYASHI S, MORIZUMI S, ABE S, OKAZAKI H, CHEN Y, GOTO H, AONO Y, OGAWA H. Anti-fibrotic efficacy of nintedanib in pulmonary fibrosis via the inhibition of fibrocyte activity. Respiratory research. 2017b;18:1–11.

SEBTI SM, SRIMATKANDADA MIGNANO,JE,JANI,JP, S. & LAZO JS. Bleomycin hydrolase: molecular cloning, sequencing, and biochemical studies reveal membership in the cysteine proteinase family. Biochemistry. 1989;28:6544–8.

SEGEL MJ, IZBICKI G, OR COHEN,PY, WALLACH-DAYAN RCHRISTENSEN,TG, S. B. & BREUER R. Role of interferon-γ in the evolution of murine bleomycin lung fibrosis. American Journal of Physiology-Lung Cellular Molecular Physiology. 2003;285:L1255–62.

SHAKER OG, SOUROUR DA. Effect of leukotriene receptor antagonists on lung fibrosis in rats. J Appl Toxicol. 2011;31:678–84.

SHEPPARD D. The role of integrins in pulmonary fibrosis. European Respiratory Review. 2008;17:157–62.

SISSON TH, MENDEZ M, CHOI K, SUBBOTINA N, CUNNINGHAM COUREY,A, DAVE A, LIU AENGELHARDT,JF, X. & WHITE ES. Targeted injury of type II alveolar epithelial cells induces pulmonary fibrosis. Am J Respir Crit Care Med. 2010;181:254–63.

STARCH C, LACTOSE ES. OIL, L. M., ACID, S. & SUCROSE, S. A. Medrol®.

SWARTZ SL, DLUHY RG. Corticosteroids: clinical pharmacology and therapeutic use. Drugs. 1978;16:238–55.

THANNICKAL VJ, HOROWITZ JC. 2006. Evolving concepts of apoptosis in idiopathic pulmonary fibrosis. *Proceedings of the American Thoracic Society*, 3, 350–356.

TODD NW, IACONO SCHERAGA,RG,GALVIN,JR, BRITT AT, E. J., LUZINA, I. G., BURKE, A. P. & ATAMAS, S. P. 2013. Lymphocyte aggregates persist and accumulate in the lungs of patients with idiopathic pulmonary fibrosis. *Journal of inflammation research*, 6, 63.

TOUTAIN P, KORITZ G, FAYOLLE P, ALVINERIE M. Pharmacokinetics of methylprednisolone, methylprednisolone sodium succinate, and methylprednisolone acetate in dogs. Journal of pharmaceutical sciences. 1986;75:251–5.

TSOUTSOU PG, PETINAKI GOURGOULIANIS,KI, GERMENIS E, MPAKA ATSOUTSOU,AG, M., EFREMIDOU, S. & MOLYVDAS P-A. 2006. Cytokine levels in the sera of patients with idiopathic pulmonary fibrosis. *Respiratory medicine*, 100, 938–945.

UBIETA K, THOMAS, M. J. & WOLLIN L. The Effect of Nintedanib on T-Cell Activation, Subsets and Functions. Drug Design Development Therapy. 2021;15:997.

VANCHERI C, KREUTER M, RICHELDI L, RYERSON CJ, VALEYRE D, WIEBE GRUTTERS,JC, QUARESMA SSTANSEN,W, M. & STOWASSER S. Nintedanib with add-on pirfenidone in idiopathic pulmonary fibrosis. Results of the INJOURNEY trial. Am J Respir Crit Care Med. 2018;197:356–63.

VARONE F, SGALLA G, IOVENE B, BRUNI T, RICHELDI L. Nintedanib for the treatment of idiopathic pulmonary fibrosis. Expert opinion on pharmacotherapy. 2018;19:167–75.

VASARMIDI E, TSITOURA E, SPANDIDOS DA, TZANAKIS N, ANTONIOU KM. Pulmonary fibrosis in the aftermath of the COVID-19 era. Experimental therapeutic medicine. 2020;20:2557–60.

VET—QL01DC01, A. 1983. Bleomycin Sulfate (USAN, pINNM). *drugs*, 17, 532-8.

WILLIAMSON JD, SADOFSKY, L. R. & HART SP. The pathogenesis of bleomycin-induced lung injury in animals and its applicability to human idiopathic pulmonary fibrosis. Experimental lung research. 2015;41:57–73.

WILSON M, WYNN T. Pulmonary fibrosis: pathogenesis, etiology and regulation. Mucosal immunology. 2009;2:103–21.

WOLLIN L, MAILLET I, QUESNIAUX V, RYFFEL B. Nintedanib reduces bleomycin-induced lung inflammation and fibrosis in mice. Eur Respiratory Soc; 2013.

WOLLIN L, WEX E, PAUTSCH A, SCHNAPP G, HOSTETTLER KE, STOWASSER S, KOLB M. Mode of action of nintedanib in the treatment of idiopathic pulmonary fibrosis. Eur Respir J. 2015;45:1434–45.

WUYTS WA, AGOSTINI C, ANTONIOU KM, BOUROS D, COTTIN CHAMBERS,RC, LORIES VEGAN,JJ,LAMBRECHT,BN, R. & PARFREY H. The pathogenesis of pulmonary fibrosis: a moving target. Eur Respir J. 2013;41:1207–18.

WYNN TA. Integrating mechanisms of pulmonary fibrosis. J Exp Med. 2011;208:1339–50.

YOULE RJ, STRASSER A. The BCL-2 protein family: opposing activities that mediate cell death. Nature reviews Molecular cell biology. 2008;9:47–59.

ZAKARIA DM, ZAHRAN NM, ARAFA, S. A. A., MEHANNA, R. A. & ABDEL-MONEIM RA. Histological and physiological studies of the effect of bone marrow-derived mesenchymal stem cells on bleomycin induced lung fibrosis in adult albino rats. Tissue engineering regenerative medicine. 2021;18:127–41.

ZHANG C, WU Z, LI JW, TAN K, YANG W, ZHAO H, WANG GQ. Discharge may not be the end of treatment: Pay attention to pulmonary fibrosis caused by severe COVID-19. Journal of medical virology. 2021;93:1378–86.

ZHAO L, MU B, CHENG ZHOU,R, Y. & HUANG C. Iguratimod ameliorates bleomycin-induced alveolar inflammation and pulmonary fibrosis in mice by suppressing expression of matrix metalloproteinase-9.

Int J Rheum Dis. 2019;22:686–94.

ZHOU Y, HUANG X, KURUNDKAR HECKER,L, KURUNDKAR D, LIU A, DESAI HJIN,T-H, L., BERNARD, K. & THANNICKAL VJ. Inhibition of mechanosensitive signaling in myofibroblasts ameliorates experimental pulmonary fibrosis. J Clin Investig. 2013;123:1096–108.

ZISMAN DA, KEANE MP, BELPERIO, J. A., STRIETER, R. M. & LYNCH JP. 2005. Pulmonary fibrosis. *Fibrosis Research*, 3–44.

Figures

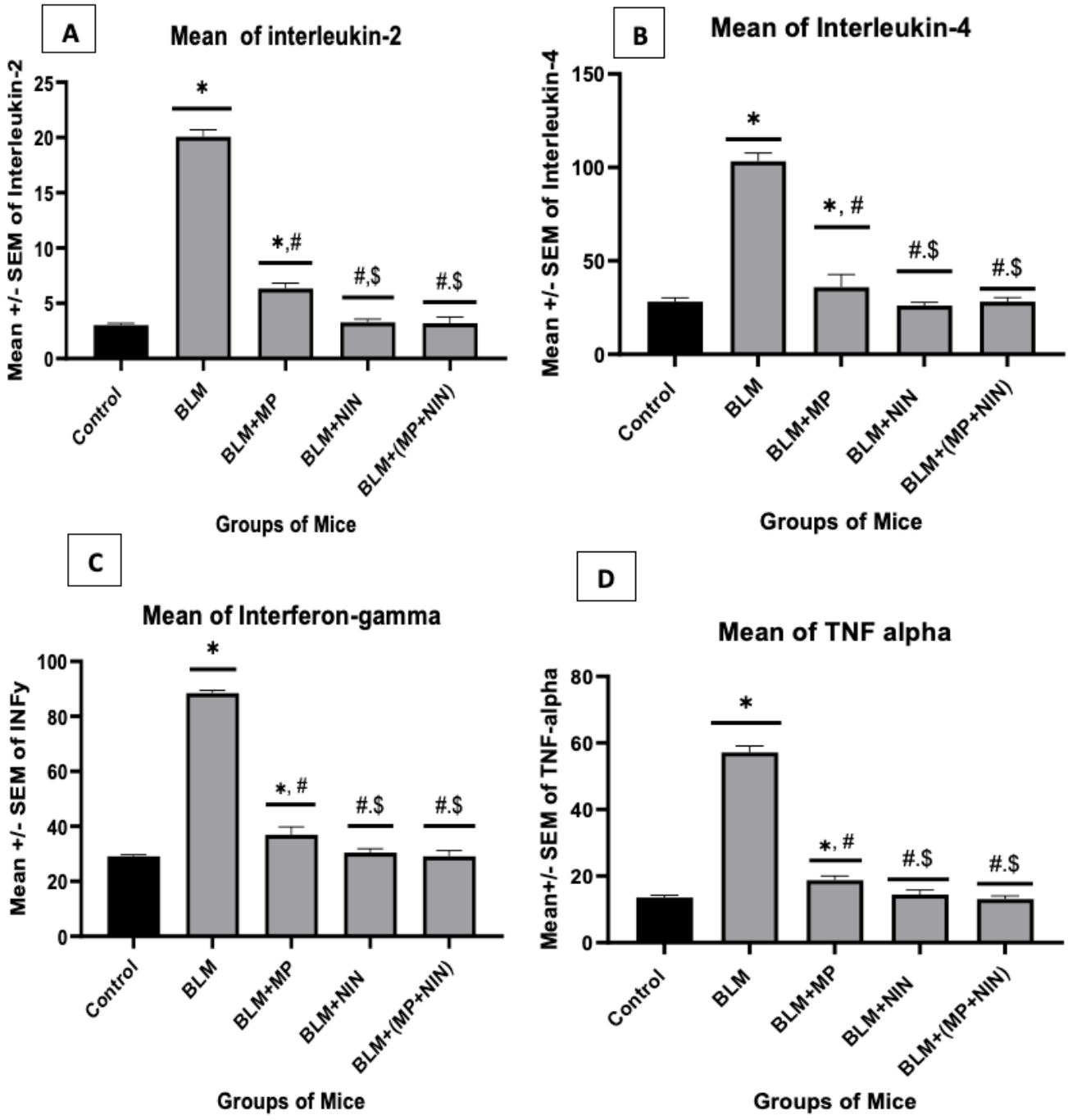

Figure 1

showed the effect of nintedanib and methylprednisolone either alone or in combination on inflammatory markers and cytokines contents in lung tissue in a mice model of corticosteroid resistance pulmonary fibrosis induced by bleomycin 7-days post treatments. A: Interleukin-2, B: Interleukin-4, C: Interferon-gamma, D: Tumor Necrosis Factor-α. Data Values were mean ± standard error of mean (SEM); N = number of animals. BLM; bleomycin, MP; methylprednisolone, NIN; nintedanib. (%) = mean percentage change compared to control group. ANOVA one-way, accompanied by a multiple comparison test by Tukey. * Control group compared to other groups. # BLM group compared to treatments group. $ BLM+MP group compared to BLM+NIN and BLM+(MP+NINI). @ BLM+NIN compared to BLM+ (MP + NIN) group.

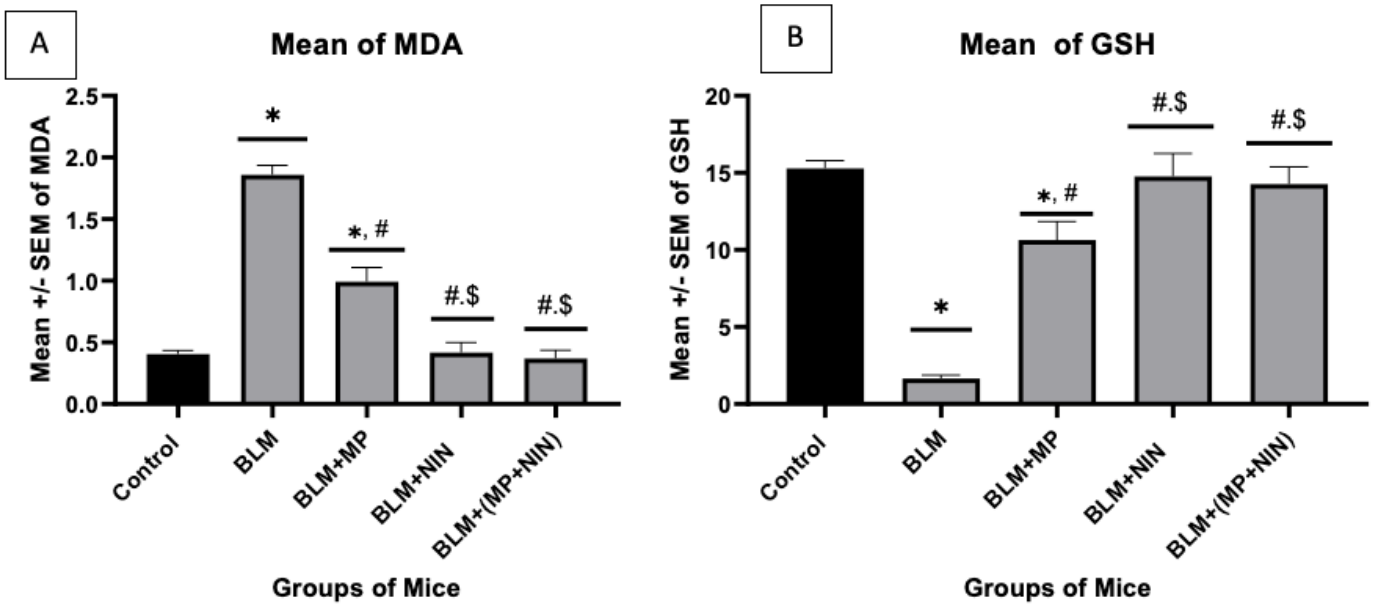

Figure 2

showed the effect of nintedanib either alone or in combination with methylprednisolone on level of MDA & GSH in lung tissue on corticosteroid resistance pulmonary fibrosis resistance to corticosteroid. Data Values were mean ± standard error of mean (SEM); N = number of animals. BLM; bleomycin, MP; methylprednisolone, NIN; nintedanib. (%) = mean percentage change compared to control group. ANOVA one-way, accompanied by a multiple comparison test by Tukey. * Control group compared to other groups. # BLM group compared to treatments group. $ BLM+MP group compared to BLM+NIN and BLM+(MP+NINI). @ BLM+NIN compared to BLM+ (MP + NIN) group.

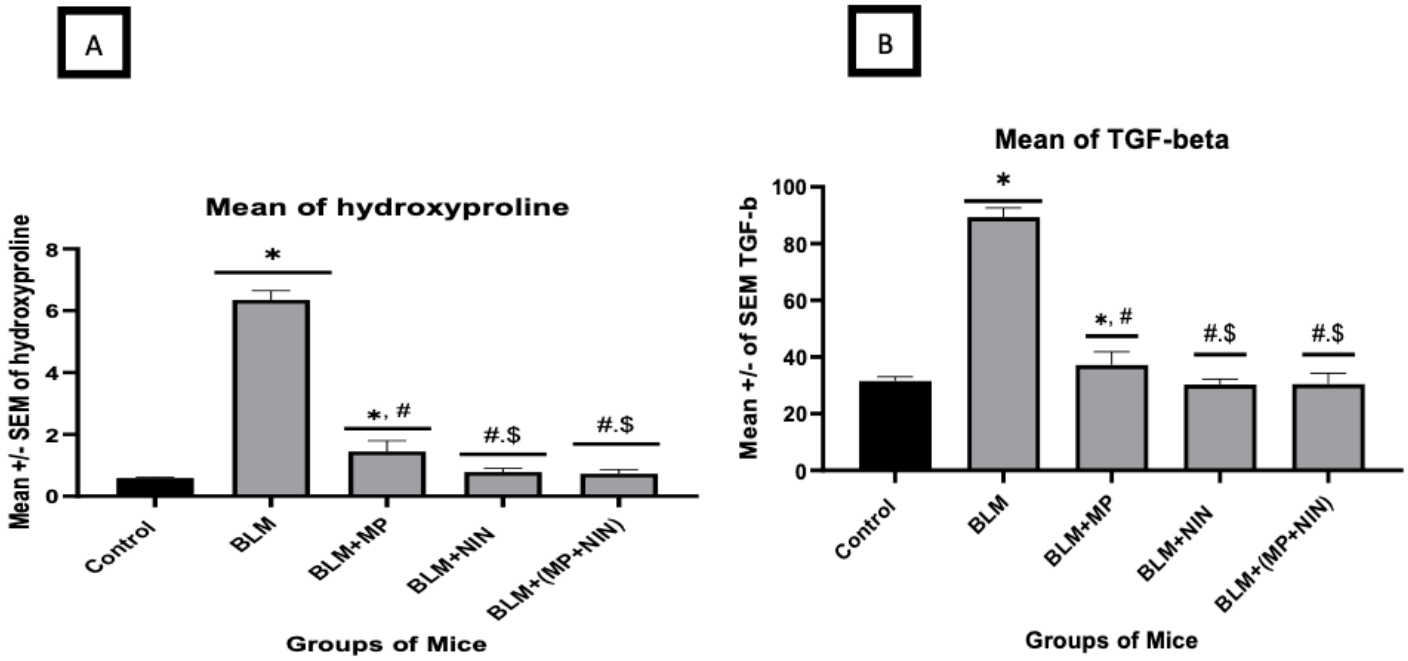

Figure 3

showed the effect of nintedanib either alone or in combination with methylprednisolone on level of TGF-β & hydroxyproline in lung tissue on corticosteroid resistance pulmonary fibrosis resistance to corticosteroid. Data Values were mean ± standard error of mean (SEM); N = number of animals. BLM; bleomycin, MP; methylprednisolone, NIN; nintedanib. (%) = mean percentage change compared to control group. ANOVA one-way, accompanied by a multiple comparison test by Tukey. * Control group compared to other groups. # BLM group compared to treatments group. $ BLM+MP group compared to BLM+NIN and BLM+(MP+NINI). @ BLM+NIN compared to BLM+ (MP + NIN) group

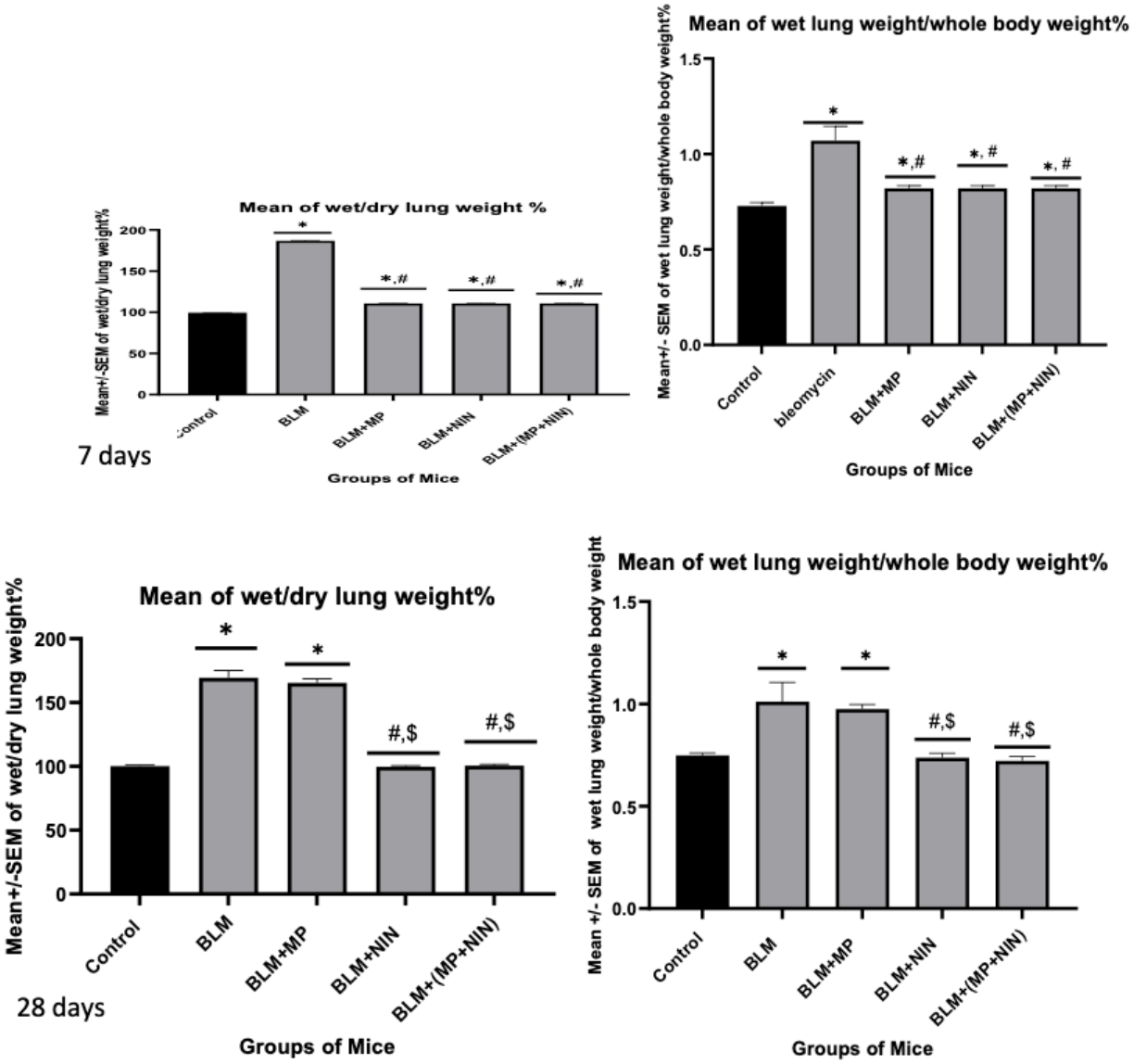

Figure 4

showed the effect of nintedanib and methylprednisolone either alone or in combination on the lung water content in lung tissue in a mice model of corticosteroid resistance pulmonary fibrosis induced by bleomycin after seven (7) & 28 days post treatments Data Values were mean ± standard error of mean (SEM); N = number of animals. BLM; bleomycin, MP; methylprednisolone, NIN; nintedanib. (%) = mean percentage change compared to control group. ANOVA one-way, accompanied by a multiple comparison test by Tukey. * Control group compared to other groups. # BLM group compared to treatments group. $ BLM+MP group compared to BLM+NIN and BLM+(MP+NINI). @ BLM+NIN compared to BLM+ (MP + NIN) group

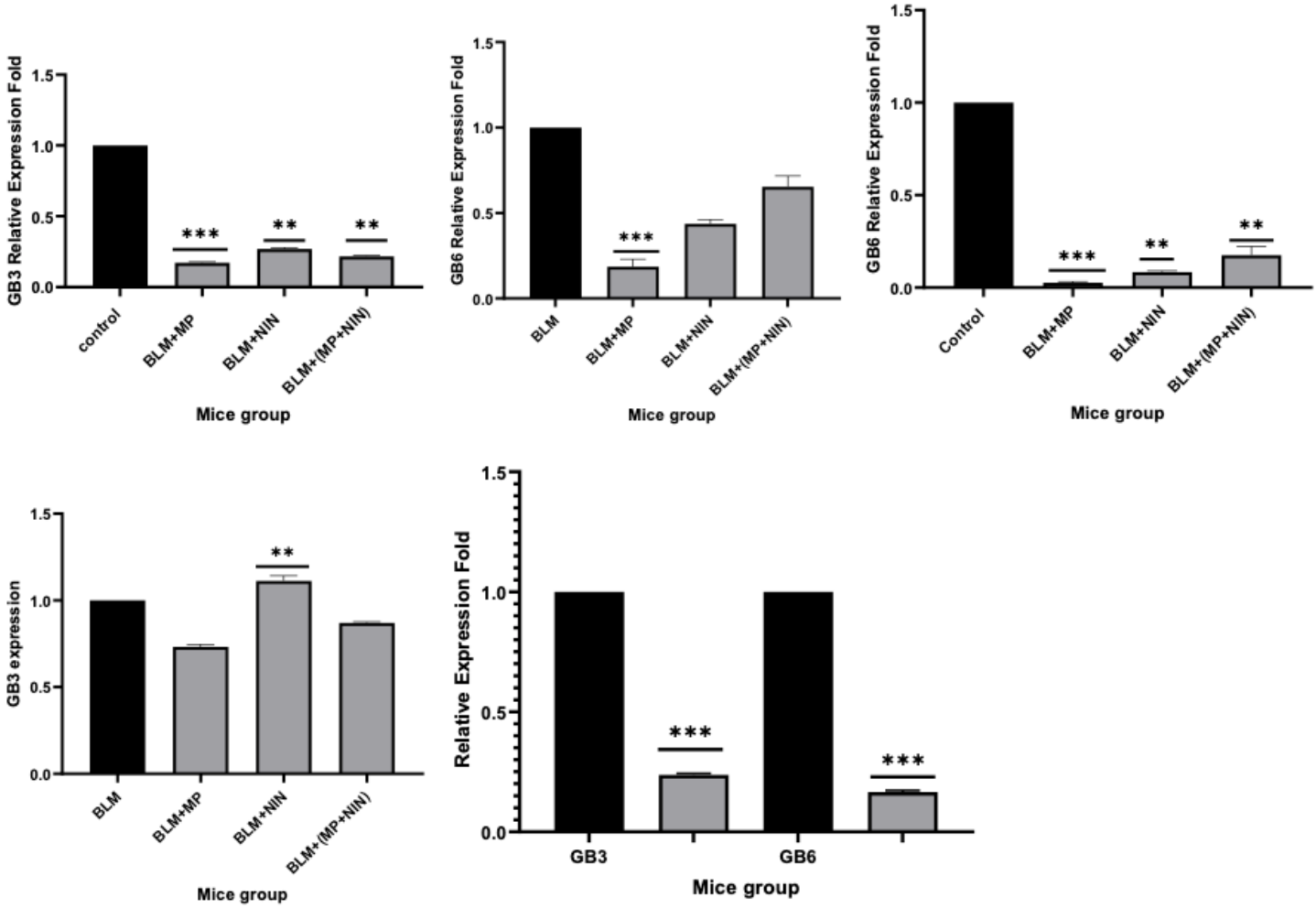

Figure 5

showed the effect of nintedanib (NIN) and methylprednisolone (MP) either alone or in combination on gene expression of β3 & β 6 integrin compared to control group and bleomycin group in lung tissue in a mice model of corticosteroid resistance pulmonary fibrosis induced by bleomycin 28 days post treatments. Data Values were mean ± standard error (SEM). BLM; bleomycin, MP; methylprednisolone, NIN; nintedanib. Student's t-test for paired comparisons was performed. The log2-transformed data was used for the RT-qPCR statistical analysis. *** very. Significant at value < 0.000, ** significant at p. value< 0.01.

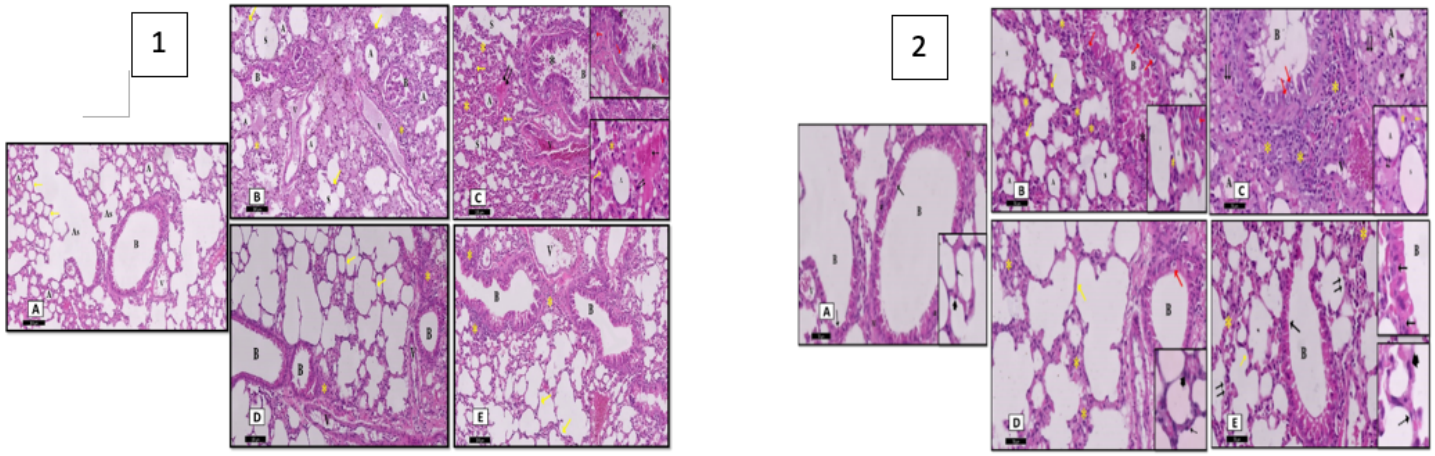

Figure 6

(1) A photomicrograph of the histology (H&E x 10; scale bar 100 µm): A (control group) displaying the normal lung architecture; expanded alveoli (A) and alveolar sacs (As) separated by thin interalveolar septa (yellow arrow), bronchioles (B) and a nearby pulmonary blood vessels (V). B (BLM group): obliterated bronchiole (B) by detached epithelial cells, heavy cellular infiltration (yellow *) in the interstitial tissue and surrounding the bronchiole, markedly thickened inter-alveolar septa (yellow arrow), and congested with thickened wall blood vessel (V) are seen. Notice obliteration of most alveoli with some alveoli appear collapsed (A) and widening of other alveoli (s). C (BLM+ MP group): collapsed alveoli (A) wall, heavy cellular infiltration (yellow *), markedly thickened inter-alveolar septa (yellow arrow), and partially obliterated bronchiole (B) by detached epithelial cells (black *), dilated congested and thickened blood vessel (V). Notice eosinophilic exudate (↑↑) in the septa and around alveoli. D (BLM+NIN group) & E (BLM+MP+NIN group): most of the bronchiolar (B) epithelial lining are normal as compared to that of group II and group III with dilated blood vessel (V). Most of the alveoli show thin interalveolar septa (yellow arrow) and some with inflammatory cell infiltration (yellow*) near to the bronchiole. (2) photomicrograph of the histology (H&E x 20; scale bar 50 µm): A (control group): two adjacent bronchioles (B) lined by simple columnar partially ciliated epithelium, a thin layer of smooth muscle fiber (M) and adventitia (a). Clara cells are present in between the lining cells with their dome shaped apices (black↑). Expanded alveoli (A) separated by thin interalveolar septa. The alveoli lined by thin pneumocytes type I (dot arrow) with flat nucleus and cuboidal pneumocytes type II (arow head) with rounded nuclei project to alveoli lumen. B (BLM group): a lumen of the bronchiolar passage (B) fill with cellular debris and inflammatory cells (black *). The epithelial lining appears vacuolated with darkly stained nuclei (red ↑). Notice markedly thickened inter-alveolar septa (yellow arrow) and heavy cellular infiltration (yellow *) are seen. Notice some alveoli appear collapsed (A) and widening of other alveoli (s). C (BLM + MP group): the epithelial lining of the bronchiolar passage (B) appears vacuolated with eukaryotic nucleus (red ↑) with multiple area of eosinophilic red materials (↑↑). Notice congested dilated with thickened wall blood vessel (V), markedly thickened inter-alveolar septa (yellow arrow), and heavy cellular infiltration (yellow *) around the bronchiole are seen. Notice marked obliteration of most alveoli, some collapsed (A) and widening of other alveoli (s) appear. D (BLM+NIN group): most of the bronchiolar

(B) epithelial lining are normal as compared to that of group II and group III with few vacuolated cells (red ↑). The alveoli are mostly lined by the thin type I pneumocyte (dot arrow) with their flat nuclei and pneumocytes type II (arow head). Some areas show thin interalveolar septa (yellow arrow) and some with inflammatory cell infiltration (yellow*) in thickened interalveolar septa. E (BLM+MP+NIN group): apparently normal bronchiolar (B) epithelial lining as compared to that of group II and group III. Clara cells are present in between the lining cells with their dome shaped apices (black↑). The alveoli are mostly lined by the thin type I pneumocyte (dot arrow) with their flat nuclei and pneumocytes type II (arow head). Some areas show thin interalveolar septa (yellow arrow) and some with thickened interalveolar septa (↑↑) with few areas of inflammatory cell infiltration (yellow*).

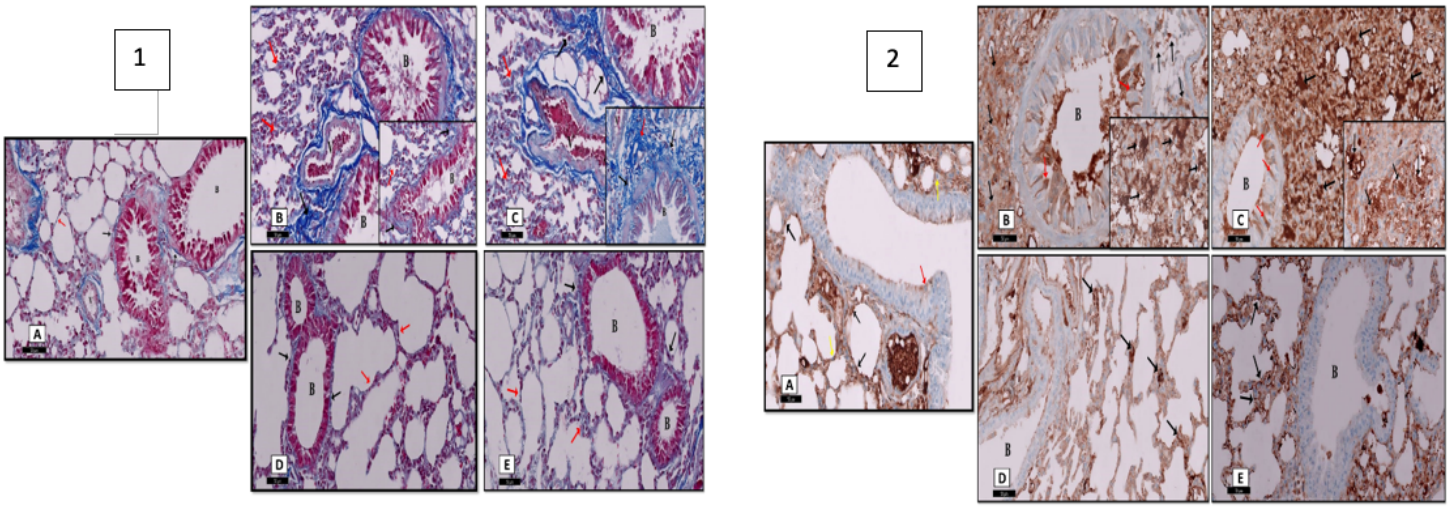

Figure 7

(1) Masson trichrome stained X 20; scale bar 50μm section of a mouse lung after 7 days showing A (control group): few collagen fibers in the interalveolar septa (red ↑), around the bronchiole (black ↑) and surrounding mainly the walls of the blood vessels (V). B (BLM group): marked collagen fibers deposition around alveoli (red ↑), bronchiole (black ↑), and blood vessel (V). C (BLM+MP group): marked collagen fibers deposition around alveoli (red ↑), bronchiole (black ↑), and blood vessel (V). D (BLM+NIN group) &E (BLM+(MP+NIN) group): few collagen fibers in the interalveolar septa (red ↑) and around the bronchiole (black ↑). (2) Immunohistochemical staining for BCL-2 x 10; scale bar 50 μm of a section in the lung of a mouse lung after 7 days showing: A (control group): weak BCL-2 positive brownish expression of the cytoplasm of alveolar lining (yellow arrow) and bronchiolar epithelium (red arrow). Notice strong positive reaction in the interstitial tissue (black arrow). B (BLM group): massive strong BCL-2 positive brownish expression of the cytoplasm of the cells in the interstitial tissue (black arrow) and few positive cells lining the bronchiole (red arrow). C (BLM+MP group): massive strong BCL-2 positive brownish expression of the cytoplasm of the cells in the interstitial tissue (black arrow) and few positive cells lining the bronchiole (red arrow). D (BLM+NIN group) &E (BLM+MP+NIN group): negative BCL-2 positive brownish expression of the cytoplasm of bronchiolar epithelium (red arrow). Notice few strong positive reactions in the interstitial tissue (black arrow).

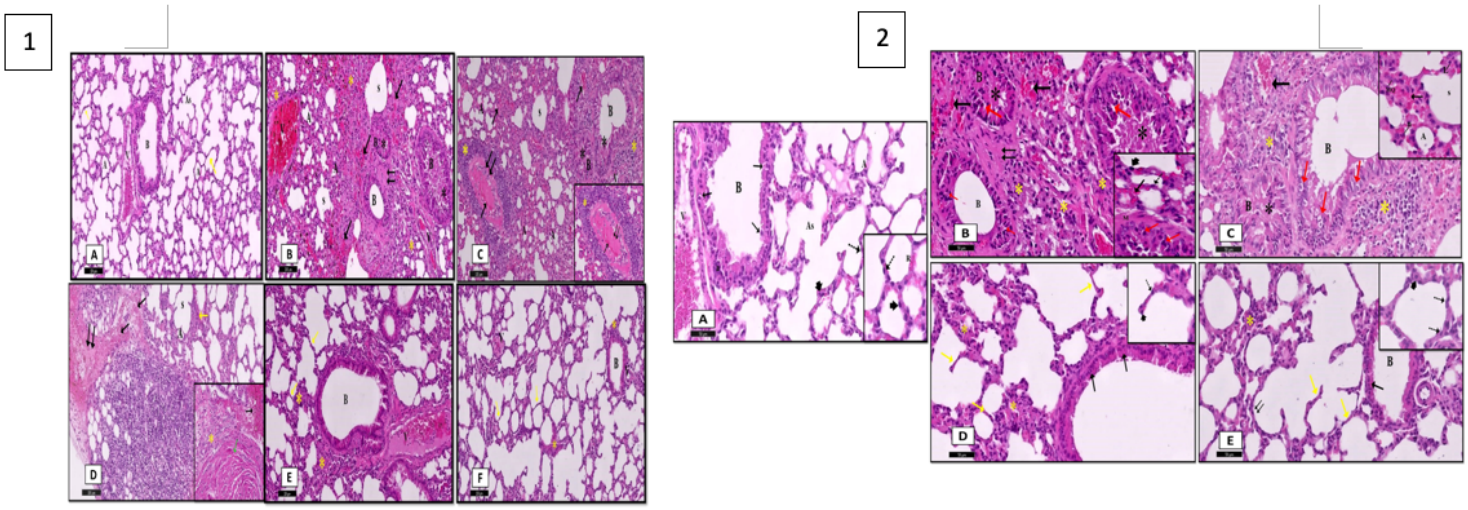

Figure 8

(1) A photomicrograph of histology (H&E x 10; scale bar 100 µm): A (control group): displaying the normal lung architecture; expanded alveoli (A) and alveolar sacs (As) separated by thin interalveolar septa (yellow arrow), bronchioles (B) and a nearby pulmonary blood vessels (V). B (BLM group): marked loss of architecture of the bronchiole (B) and cellular debris in the lumen (black *), marked inflammatory cellular infiltration (yellow *) in the interstitial tissue and surrounding the bronchiole, and congested dilated blood vessel (V) are seen. Notice obliteration of most alveoli with some alveoli appear collapsed (A) and widening of other alveoli (s). Marked eosinophilic exudate (↑↑) in the septa and around alveoli and many extravasations of RBCs (↑). C (BLM+MP group): narrowing of some alveoli (A) and over dilatation of others (s). Notice eosinophilic exudate (↑↑) in the septa and around alveoli and many extravasations of RBCs (↑) with heavy cellular infiltration (yellow *) surrounding the bronchiole and the eosinophilic exudate. Partially obliterated bronchiole (B) by detached epithelial cells (black *). D (BLM+MP) (another section): marked cellular acidophilic lugs with spindle shape (green arrow), marked eosinophilic exudate (↑↑) with focal rounded zone of inflammatory cells (yellow*), thickened inter-alveolar septa (yellow arrow), and many extravasations of RBCs (↑) are seen. E (BLM+NIN group) &F (BLM+(MP+NIN) group): most of the bronchiolar (B) epithelial lining are normal as compared to that of group II and group III with a nearby blood vessels (V). Most of the alveoli show thin interalveolar septa (yellow arrow) and some with focal inflammatory cell infiltration (yellow*) near to the bronchiole. (2) A photomicrograph of histology (H&E x 20; scale bar 50 µm): A (control group): bronchiole (B) lined by simple columnar partially ciliated epithelium, a thin layer of smooth muscle fiber (M) and adventitia (a). Clara cells are present in between the lining cells with their dome shaped apices (black↑). Expanded alveoli (A) separated by thin interalveolar septa. The alveoli lined by thin pneumocytes type I (dot arrow) with flat nucleus and cuboidal pneumocytes type II (arow head) with rounded nuclei project to alveoli lumen. B (BLM group): a lumen of the bronchiolar passage (B) fill with cellular debris and inflammatory cells (black *) with thick muscle layer (M). The epithelial lining appears vacuolated with darkly stained nuclei (red ↑). Notice markedly thickened inter-alveolar septa studded with heavy cellular infiltration (yellow *) are seen. Notice pneumocytes type I (dot arrow) and cuboidal pneumocytes type II (arow head)

appear with deeply stained pyknotic nuclei. The eosinophilic exudate (↑↑) and many extravasations of RBCs (black ↑) are seen. C (BLM+MP group): the epithelial lining of the bronchiolar passage (B) appears vacuolated with eukaryotic nucleus (red ↑) with multiple area of eosinophilic red materials (↑↑). Notice extravasations of RBCs (black↑), and heavy cellular infiltration (yellow *) in the form of lymphocytes (L), neutrophil (n), and multinucleated giant cells (MQ) in thickened interalveolar septa around the alveoli are seen. Notice marked obliteration of most alveoli, some collapsed (A) and widening of other alveoli (s) appear. D (BLM+NIN group) &E (BLM+(MP+NIN) group): apparently normal bronchiolar (B) epithelial (black↑) lining as compared to that of group II and group III. The alveoli are mostly lined by the thin type I pneumocyte (dot arrow) with their flat nuclei and pneumocytes type II (arow head). Most of the lung section show thin interalveolar septa (yellow arrow) and some with thickened interalveolar septa (↑↑) with few focal areas of inflammatory cell infiltration (yellow*).

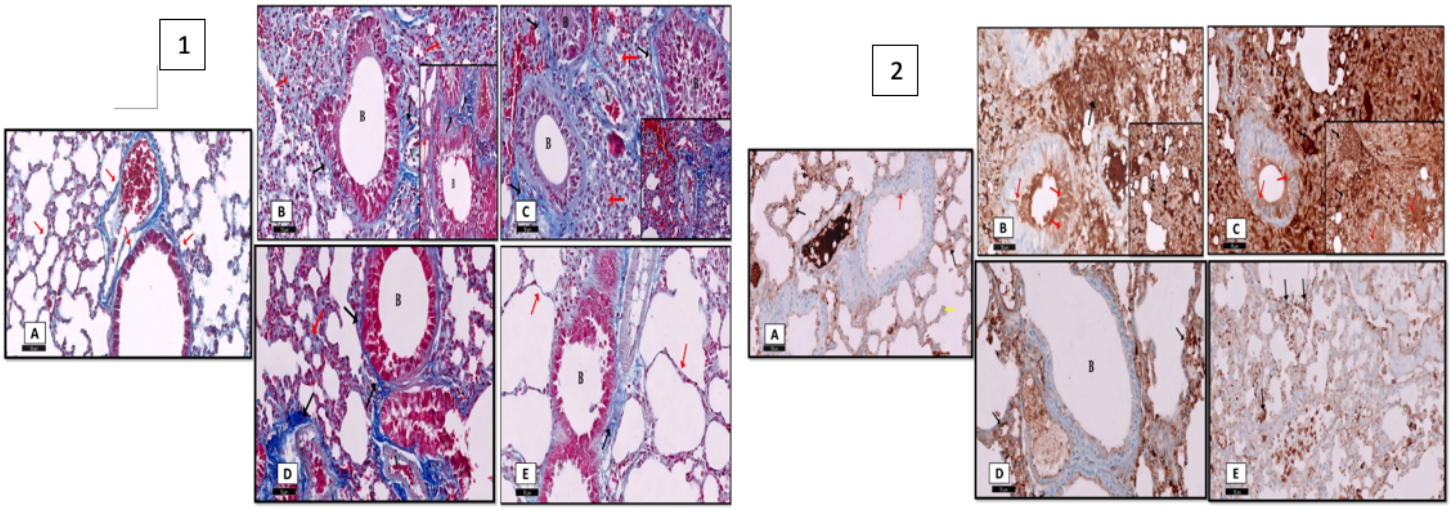

Figure 9

(1) Masson trichrome stained x 20; scale bar 50 µm section of a mouse lung after 28 days showing: A (control group): few collagen fibers in the interalveolar septa (red ↑), around the bronchiole (black ↑) and surrounding mainly the walls of the blood vessels (V). B (BLM group): marked collagen fibers deposition around alveoli (red ↑), bronchiole (black ↑), and blood vessel (V). C (BLM+MP group): marked collagen fibers deposition around alveoli (red ↑), bronchiole (black ↑), and blood vessel (V). D (BLM+NIN group): few collagen fibers in the interalveolar septa (red ↑) and around the bronchiole (black ↑). E (BLM+ (MP+NIN) group): few collagen fibers in the interalveolar septa (red ↑) and around the bronchiole (black ↑). (2) Immunohistochemical staining for BCL-2 x10; scale bar 50 µm of a section in the lung of a mouse lung after 28 days showing: A: (control group): weak BCL-2 positive brownish expression of the cytoplasm of alveolar lining (yellow arrow) and bronchiolar epithelium (red arrow). Notice strong positive reaction in the interstitial tissue (black arrow). B (BLM group): massive strong BCL-2 positive brownish expression of the cytoplasm of the cells in the interstitial tissue (black arrow) and few positive cells lining the bronchiole (red arrow). C (BLM+MP group): massive strong BCL-2 positive brownish expression of the cytoplasm of the cells in the interstitial tissue (black arrow) and few positive cells lining the bronchiole (red arrow). D (BLM+NIN group): negative BCL-2 positive brownish expression of the cytoplasm of

bronchiolar epithelium (red arrow). Notice few strong positive reactions in the interstitial tissue (black arrow). E (BLM+(MP+NIN) group): few strong positive reactions in the interstitial tissue (black arrow).